

Constructing Galerkin's Approximations of Invariant Tori Using MACSYMA*

DAVID E. GILSINN

Manufacturing Engineering Laboratory, Bldg. 233, B106, National Institute of Standards and Technology, Gaithersburg, MD 20899, U.S.A.

(Received: 28 January 1994; accepted: 22 July 1994)

Abstract. Invariant tori of solutions for nonlinearly coupled oscillators are generalizations of limit cycles in the phase plane. They are surfaces of aperiodic solutions of the coupled oscillators with the property that once a solution is on the surface it remains on the surface. Invariant tori satisfy a defining system of nonlinear partial differential equations. This case study shows that with the help of a symbolic manipulation package, such as MACSYMA, approximations to the invariant tori can be developed by using Galerkin's variational method. The resulting series must be manipulated efficiently, however, by using the Poisson series representation for multiply periodic functions, which makes maximum use of the list processing techniques of MACSYMA. Three cases are studied for the single van der Pol oscillator with forcing parameter $\varepsilon = 0.5, 1.0, 1.5$, and three cases are studied for a pair of nonlinearly coupled van der Pol oscillators with forcing parameters $\varepsilon = 0.005, 0.5, 1.0$. The approximate tori exhibit good agreement with direct numerical integrations of the systems.

Key words: Galerkin's method, invariant tori, Poisson series, symbolic manipulation, van der Pol oscillator.

1. Introduction

Many authors have considered the problem of approximating the limit cycle of the van der Pol oscillator

$$\ddot{z} + \omega^2 z = \varepsilon(1 - z^2)\dot{z}. \quad (1)$$

Of those, several have developed series representations of the limit cycle for various values of the parameter ε using both perturbation and Galerkin methods. Loud [29] developed a first order parametric representation of (1) forced by $0.1 \cos(t)$ with $\varepsilon = 3.0$ using the properties of invariant manifolds. Stokes [40] extended the nonlinear Galerkin methods of Urabe [42] to autonomous differential equations and developed a series representation up to the seventh harmonic for the case $\varepsilon = 0.1$. Others have used Poincaré–Lindstedt methods. Melvin [32, 33] describes a computer implementation of the Poincaré–Lindstedt method for $0 \leq \varepsilon \leq 1.5$. Deprit and Schmidt [11] complemented Melvin's work by symbol manipulation to develop an exact representation for the limit cycle and its frequencies up to ε^8 . Other series methods have also been attempted. The author [21], using methods of integral manifolds, developed a parametric representation of the limit cycle. Garcia-Margallo and Bejarano [19] developed a first order solution by the method of harmonic balance for a generalized van der Pol oscillator with $\varepsilon = 0.1$.

The dynamics of mutually coupled van der Pol oscillators have also been studied by a number of authors. Rand and Holmes [35] have studied them with weakly diffuse linear

* Contribution of the National Institute of Standards and Technology, a Federal agency. Not subject to copyright.

coupling. They look for conditions that lead to phase-locked periodic solutions using a two-time expansion technique. Storti and Rand [41] have extended this work to the case of strong diffuse linear coupling. Kouda and Mori [27] have used nonlinear modal analysis to study the stability of various modes for a system of mutually coupled van der Pol oscillators with fifth order nonlinear characteristics and coupling delay. All of these studies, however, have looked at particular time dependent solutions.

When two van der Pol oscillators are coupled nonlinearly the solutions can form a surface of solutions called an invariant torus. Very few authors have approached the problem of approximating an entire invariant torus for coupled van der Pol oscillators. Diliberto *et al.* [14] related the construction of invariant tori (or periodic surfaces in their terminology) to the construction of first integrals. Diliberto [13] developed a formal iterative technique of developing a periodic surface by generating sequences of near-identity transformations. He suggested that this technique could be applied to non-Hamiltonian systems. However, no application was given to a particular system. The author, Gilsinn [22], proposed a technique for directly computing invariant tori for weakly nonlinearly coupled oscillators and showed that it could approximate the motion of two nonlinearly coupled van der Pol oscillators on the torus to a high degree of accuracy but only under the assumption of small ε . Dieci *et al.* [12] have recently developed a numerical scheme to approximate tori but do not give direct analytic representations.

The current work is a case study of the computational experience involved in applying both symbolic and numerical methods to the construction of analytic representations of invariant tori for a larger range of ε . The goal of producing a parametric representation of a torus is of course to reduce the order of the system being solved. The Galerkin method is used along with standard trigonometric basis functions in order to study large nonlinearities. This report shows, in Section 2, that the construction of a parametric representation of an invariant torus for a system of coupled oscillators of the form

$$\begin{aligned}\ddot{z}_1 + \omega_1^2 z_1 &= \varepsilon f_1(\mathbf{z}, \dot{\mathbf{z}}), \\ \ddot{z}_2 + \omega_2^2 z_2 &= \varepsilon f_2(\mathbf{z}, \dot{\mathbf{z}}),\end{aligned}\tag{2}$$

where $\mathbf{z} = (z_1, z_2)^T$, $\dot{\mathbf{z}} = (\dot{z}_1, \dot{z}_2)^T$, $\varepsilon > 0$, can be reduced to the construction of a solution of a system of partial differential equations in a similar manner to the construction of center manifolds as described by Carr [6]. The general form of the Galerkin projection equations is then developed. The construction of invariant tori and other invariant manifolds such as inertial manifolds is related to the construction of center manifolds in Section 3. To apply the Galerkin method efficiently in a symbolic manipulation program some intermediate trigonometric representations are used, called Poisson series, described in Section 4. Not all symbolic programs provide Poisson series expansions for trigonometric series but MACSYMA does provide such a facility (see MACSYMA [30]). The demonstration of the power of this facility is the basis for the rest of this paper.

Periodic surfaces have not been the subject of much investigation due in part the author believes to the extremely large trigonometric expansions that result whereas Taylor series expansions have been successfully used to develop center manifolds. For example, Shaw and Pierre [38] have used the technique of nonlinear normal modes to develop a series representation for a center manifold by constructing a solution to an appropriate partial differential equation using methods described in Carr [6]. The use of Poisson series to represent trigonometric series, however, provides an efficient intermediate tool to investigate periodic

and quasi-periodic surfaces. In Section 5 Galerkin constructions, using Poisson series as a tool, will be given for the limit cycle of the van der Pol oscillator and the invariant torus of a nonlinearly coupled system of van der Pol oscillators. A typical MACSYMA program to compute the torus approximation will be given in Section 6 and a discussion of some interesting properties of the residual errors between predicted and computed trajectories on the torus will be examined in Section 7 while some final conclusions will be given in Section 8.

2. A System of Partial Differential Equations

One of the first steps in transforming the problem of computing an invariant torus for (2) into the problem of solving a system of partial differential equations is to introduce polar coordinates

$$\begin{aligned} z_j &= x_j^\gamma \sin \omega_j \theta_j, \\ \dot{z}_j &= \omega_j x_j^\gamma \cos \omega_j \theta_j, \end{aligned} \tag{3}$$

for $j = 1, 2$, where $\gamma > 0$ is introduced to simplify powers if necessary. Using (3) it is not hard to show that (2) can be reduced to a system of the form

$$\begin{aligned} \dot{\theta} &= \mathbf{d} + \varepsilon \Theta(\theta, \mathbf{x}), \\ \dot{\mathbf{x}} &= \varepsilon \mathbf{X}(\theta, \mathbf{x}), \end{aligned} \tag{4}$$

where $\theta = (\theta_1, \theta_2)^T$, $\mathbf{d} = (1, 1)^T$, $\Theta = (\Theta_1, \Theta_2)^T$, $\mathbf{x} = (x_1, x_2)^T$, $\mathbf{X} = (X_1, X_2)^T$. $\Theta(\theta, \mathbf{x})$, $\mathbf{X}(\theta, \mathbf{x})$ are assumed to be periodic with vector period $2\pi/\omega = (2\pi/\omega_1, 2\pi/\omega_2)$. No attempt will be made in this paper to be concerned with the minimal conditions for the existence of invariant tori. For a discussion of many of these conditions see Aulbach [1] or Hale [24]. As a result Θ , X will be assumed to be sufficiently differentiable with bounded derivatives for $\Theta \in R^2$ and $X \in D \subset R^2$, D a large but compact region in R^2 .

A parameterized surface $\mathbf{x} = \mathbf{S}(\theta)$, with vector period $2\pi/\omega$, is an invariant torus for (4), if given that $\theta(t)$ solves

$$\dot{\theta} = \mathbf{d} + \varepsilon \Theta(\theta, \mathbf{S}(\theta)), \tag{5}$$

for all $t \in (-\infty, \infty)$, then $(\theta(t), \mathbf{S}(\theta(t)))^T$ solves (4) for all $t \in (-\infty, \infty)$. To develop the partial differential equation satisfied by $\mathbf{S}(\theta)$ assume that an invariant torus for (4) exists with vector period $2\pi/\omega$. Let $\theta(t)$, with $\theta(0) = \theta$, be a solution of (5) for all $t \in (-\infty, \infty)$. Then the definition of an invariant torus implies that

$$\frac{d}{dt} (\mathbf{S}(\theta(t))) = \varepsilon \mathbf{X}(\theta(t), \mathbf{S}(\theta(t))) \tag{6}$$

or

$$D\mathbf{S}(\theta(t)) \cdot \dot{\theta}(t) = \varepsilon \mathbf{X}(\theta(t), \mathbf{S}(\theta(t))) \tag{7}$$

where $D\mathbf{S}(\theta)$ is the Jacobian given by

$$D\mathbf{S}(\theta) = \left(\frac{\partial S_i}{\partial \theta_j} \right)_{i,j=1,2} \tag{8}$$

But $\theta(t)$ solves (5) so (7) becomes

$$DS(\theta(t)) \cdot (\mathbf{d} + \varepsilon \Theta(\theta(t), \mathbf{S}(\theta(t)))) = \varepsilon \mathbf{X}(\theta(t), \mathbf{S}(\theta(t))) \tag{9}$$

or setting $t = 0$

$$DS(\theta) \cdot (\mathbf{d} + \varepsilon \Theta(\theta, \mathbf{S}(\theta))) = \varepsilon \mathbf{X}(\theta, \mathbf{S}(\theta)) \tag{10}$$

which holds true for any initial θ . (10) is the required system of partial differential equations that must be satisfied by an invariant torus. The reverse argument also shows that if $S(\theta)$ solves (10) then it is a parametric representation of an invariant torus for (4). For the sake of notation rewrite (10) as

$$(NS)(\theta) = DS(\theta) \cdot (\mathbf{d} + \varepsilon \Theta(\theta, \mathbf{S})) - \varepsilon \mathbf{X}(\theta, \mathbf{S}) = \mathbf{0}. \tag{11}$$

In this paper the Galerkin method will be applied to (11) to solve for invariant tori. The difference between this system and an analogous system used to compute center manifolds for equilibria is that in (11) vector periodic representations for $\mathbf{S}(\theta)$ are sought rather than algebraic representation. This introduces computational complexity as will become evident.

To begin the Galerkin approximation assume a trial solution of the form

$$\mathbf{S}_K(\theta) = c_1 \phi_1(\theta) + \dots + c_K \phi_K(\theta) \tag{12}$$

where $\{\phi_i(\theta)\}$ is a basis set, each $\phi_i(\theta)$ periodic with vector period $2\pi/\omega$. The parameters c_1, \dots, c_K are selected to satisfy

$$\left\langle N \left(\sum_{i=1}^K c_i \phi_i(\theta) \right), \phi_j(\theta) \right\rangle = 0 \tag{13}$$

for $j = 1, \dots, K$, where $\langle \cdot, \cdot \rangle$ is an appropriately defined inner product. System (13) is sometimes called the variational system.

In the next section we show that the problem of computing a parametric representation of an invariant torus is not an isolated problem but is linked to the problems of approximating various types of invariant manifolds. They all relate to the idea of a center manifold.

3. Invariant Manifolds

Let

$$\dot{x} = X(x) \tag{14}$$

for $x \in R^n$. A set $S \subset R^n$ is said to be an *invariant manifold* for (14) if, for $x_0 \in S$ the solution $x(t)$ of (14) with $x(0) = x_0$ is in S for all t .

A center manifold is one example of an invariant manifold. In particular, following Carr [6], consider the system

$$\begin{aligned} \dot{x} &= Ax + f(x, y), \\ \dot{y} &= By + g(x, y), \end{aligned} \tag{15}$$

where $x \in R^n, y \in R^m$. A and B are constant matrices. The eigenvalues of A have zero real parts and those of B have negative real parts. The functions f and g have continuous second

order derivatives with $f(0,0) = 0, Df(0,0) = 0, g(0,0) = 0, Dg(0,0) = 0$ where Df and Dg are Jacobian matrices. If $y = h(x)$ is an invariant manifold for (15) and h is smooth then it is called a *center manifold* if $h(0) = 0, Dh(0) = 0$. Carr [6] shows that there exists a center manifold for (15) given by $y = h(x)$ for $|x| < \delta$, where h has continuous second derivatives. In order to approximate the center manifold let $\phi: R^n \rightarrow R^m$ have continuous first derivatives in a neighborhood of the origin and define the operator

$$(N\phi)(x) = D\phi(x) \cdot (Ax + f(x, \phi)) - B\phi(x) - g(x, \phi). \tag{16}$$

This operator is analogous to that defined in (11). From the definition of a center manifold, h , it must satisfy

$$(Nh)(x) = 0. \tag{17}$$

Directly solving (17) is difficult, but the next result indicates that a center manifold can be approximated. Again, let ϕ be a continuously differentiable map of a neighborhood of the origin in R^n to R^m with $\phi(0) = 0, D\phi(0) = 0$ and suppose that as $x \rightarrow 0, (N\phi)(x) = O(|x|^q)$ where $q > 1$. Then as $x \rightarrow 0, |h(x) - \phi(x)| = O(|x|^q)$ where $q > 1$. An illustration of this calculation is given in Guckenheimer and Holmes [23]. Carr [6] has also extended these results to nonlinear wave and diffuse equations.

Nonlinear normal modes in vibration studies exhibit the properties of invariant manifolds. Shaw and Pierre [38] have used the techniques of center manifolds to show that in the neighborhood of equilibrium points nonlinear modes are invariant manifolds for nonlinear equations of motion. They begin with equations of the form

$$\begin{aligned} \dot{x}_i &= y_i, \\ \dot{y}_i &= f_i(\mathbf{x}, \mathbf{y}), \end{aligned} \tag{18}$$

for $i = 1, 2, \dots, N$ where $\mathbf{x} = (x_1, \dots, x_N)^T$ represents displacements and $\mathbf{y} = (y_1, y_2, \dots, y_N)^T$ represents the corresponding velocities. If there exists at least one motion for which all displacements and velocities are functionally related to a single pair of variables, say $u = x_1, v = y_1$, then the functional relations for the invariant manifold are assumed to be

$$\begin{aligned} x_i &= X_i(u, v), \\ y_i &= Y_i(u, v), \end{aligned} \tag{19}$$

for $i = 1, 2, \dots, N$. They show that the invariant manifold can be computed by approximating the solution of the first order partial differential equations

$$\begin{aligned} \frac{\partial X_i}{\partial u} v + \frac{\partial X_i}{\partial v} f_1(u, X_2, \dots, X_N; v, Y_2, \dots, Y_N) &= Y_i \\ \frac{\partial Y_i}{\partial u} v + \frac{\partial Y_i}{\partial v} f_1(u, X_2, \dots, X_N; v, Y_2, \dots, Y_N) &= f_i(u, X_2, \dots, X_N; v, Y_2, \dots, Y_N) \end{aligned} \tag{20}$$

by use of power series. For the problem of nonlinear normal modes (20), although written here in component form, is analogous to (10). Shaw and Pierre [39] have extended these results to nonlinear continuous systems.

Invariant manifolds in the case of quasiperiodic and periodic systems have in the past been referred to as *integral manifolds* for nonautonomous systems (see Bogoliubov and Mitropolsky [4] and Hale [24]) and *periodic surfaces* for autonomous systems (see Diliberto [13]). The results for integral manifolds are related to those of center manifolds in that they demonstrate conditions under which an equilibrium integral manifold or torus, in the case of periodic surfaces, perturbs to a nearby integral manifold or torus on which the solutions are quasiperiodic. In particular, Hale [24] extended the work of Bogoliubov and Mitropolsky [4] to a system of the form

$$\begin{aligned}\dot{\theta} &= d(\varepsilon) + \Theta(t, \theta, y, z, \varepsilon), \\ \dot{y} &= Ay + Y(t, \theta, y, z, \varepsilon), \\ \dot{z} &= \varepsilon Cz + \varepsilon Z(t, \theta, y, z, \varepsilon),\end{aligned}\tag{21}$$

and showed that there exists an integral manifold

$$\begin{aligned}y &= f(t, \theta, \varepsilon), \\ z &= g(t, \theta, \varepsilon),\end{aligned}\tag{22}$$

both quasiperiodic or periodic in t and θ depending on the quasiperiodicity or periodicity of (21). The author (Gilsinn [21]) extended the center manifold approximation theorem to one for integral manifolds by defining

$$\begin{aligned}(N_1(F, G))(t, \theta, \varepsilon) &= D_1F + D_2F \cdot [d(\varepsilon) + \Theta(t, \theta, F, G, \varepsilon)] - AF - Y(t, \theta, F, G, \varepsilon), \\ (N_2(F, G))(t, \theta, \varepsilon) &= D_1G + D_2G \cdot [d(\varepsilon) + \Theta(t, \theta, F, G, \varepsilon)] \\ &\quad - \varepsilon CG - \varepsilon Z(t, \theta, F, G, \varepsilon).\end{aligned}\tag{23}$$

If $F(t, \theta, \varepsilon)$ and $G(t, \theta, \varepsilon)$ can be constructed so that

$$\begin{aligned}|(N_1(F, G))(t, \theta, \varepsilon)| &= O(\varepsilon^N), \\ |(N_2(F, G))(t, \theta, \varepsilon)| &= O(\varepsilon^{N+1}),\end{aligned}\tag{24}$$

then

$$\begin{aligned}|f(t, \theta, \varepsilon) - F(t, \theta, \varepsilon)| &= O(\varepsilon^N), \\ |g(t, \theta, \varepsilon) - G(t, \theta, \varepsilon)| &= O(\varepsilon^N),\end{aligned}\tag{25}$$

where $f(t, \theta, \varepsilon)$ and $g(t, \theta, \varepsilon)$ are given in (22).

Some continuous dissipative systems have finite dimensional invariant manifolds called *inertial manifolds*. The evolutionary equations, when restricted to these manifolds, reduce to finite dimensional ordinary differential equations called *inertial forms*. The existence of inertial manifolds for nonlinear evolutionary equations in the self-adjoint case has been shown by Foias *et al.* [18] and in the nonself-adjoint case by Sell and You [37]. A number of authors describe methods of approximating inertial manifolds. See, for example, Brown *et al.* [5], Debussche and Marion [7], Foias *et al.* [17] and Jolly [26]. Several of these authors have used nonlinear Galerkin methods described in Marion and Temam [31]. However, the method of constructing inertial manifolds that seems closest to the approach in this paper is called elliptic

regularization, described in Fabes *et al.* [15]. In their work they are interested in the existence of inertial manifolds for nonlinear evolutionary equations of the form

$$\frac{du}{dt} + Au = F(u) \tag{26}$$

on a Hilbert space H . A is assumed to be a positive definite, self-adjoint operator on H with compact resolvent. The function F contains the nonlinear terms. They let P be an orthogonal projection of H so that the range PH is finite dimensional. If $Q = I - P$ then system (26) becomes

$$\begin{aligned} \frac{dp}{dt} + Ap &= PF(p + q) \\ \frac{dq}{dt} + Qq &= QF(p + q) \end{aligned} \tag{27}$$

where P is often selected as the projection onto the space spanned by $\{e_1, \dots, e_M\}$ where e_i is the eigenvector of the operator A corresponding to the eigenvalue λ_i , with the ordering $0 < \lambda_1 \leq \lambda_2 \leq \lambda_3 \leq \dots$. An inertial manifold is realized as the graph of a function $\Phi: PH \rightarrow OH$. If $D = \frac{\partial}{\partial p}$ denotes the derivative with respect to $p \in PH$, then Φ solves

$$D\Phi(PF(p + \Phi) - Ap) = QF(p + \Phi) - A\Phi, \tag{28}$$

a first order partial differential equation over PH . This equation is analogous to equation (10), but is solved by replacing (28) with the regularized elliptic equation

$$-\epsilon \nabla^2 \Phi + D\Phi(PF(p + \Phi) - Ap) = QF(p + \Phi) - A\Phi, \tag{29}$$

with suitable boundary conditions. Under appropriate conditions on A the solution Φ_ϵ of (29) converges to a weak solution Φ of (28) as $\epsilon \rightarrow 0$.

4. Poisson Series

For the rest of this paper we will concentrate on the quasiperiodic solutions for (10) using a special trigonometric series form for intermediate calculations because once the trial approximate solution (12) is substituted in (11) it becomes crucial that the intermediate series generated be manipulated efficiently. Jefferys [25] has pointed out that workers in celestial mechanics, constructing, for example, the theory of the orbit of a celestial body, have had to deal with expansions involving hundreds or even thousands of terms. Barton and Fitch [3] have noted that even in simple problems involving the manipulation of functions, problems starting from and resulting in quite short expressions frequently lead to intermediate expressions of inordinate length in the course of computation. They refer to this as the problem of 'blow-up'.

This problem has been somewhat alleviated by the use of a series representation called a Poisson series. This series was defined by Deprit and Rom [8] in the form

$$\begin{aligned} &\sum_{i_1 \geq 0} \sum_{i_2 \geq 0} \dots \sum_{i_m \geq 0} \sum_{j_1 \geq 0} \sum_{j_2 \neq 0} \dots \sum_{j_n \neq 0} p_1^{i_1} p_2^{i_2} \dots p_m^{i_m} \\ &\times \left[\begin{aligned} &C_{i_1, i_2, \dots, i_m}^{j_1, j_2, \dots, j_n} \cos(j_1 t_1 + j_2 t_2 + \dots + j_n t_n) \\ &+ S_{i_1, i_2, \dots, i_m}^{j_1, j_2, \dots, j_n} \sin(j_1 t_1 + j_2 t_2 + \dots + j_n t_n) \end{aligned} \right] \end{aligned} \tag{30}$$

where $i_1, i_2, \dots, i_m, j_1, j_2, \dots, j_n$ are integers, p_1, p_2, \dots, p_m are canonical, or position dependent, polynomial variables and t_1, t_2, \dots, t_n are canonical angular variables. As an example of this form of representation consider the simple expression

$$(3x^2y + x) \sin^2(v + 2) \cos^2(2v + u) \quad (31)$$

and note that it is not in the Poisson series form. However, it can be rewritten in the form

$$\begin{aligned} & -\frac{3}{8} x^2y \cos(6v + 6) - \frac{1}{8} x \cos(6v + 6u) \\ & + \frac{3}{4} x^2y \cos(4v + 2) + \frac{1}{4} x \cos(4v + 2u) \\ & - \frac{3}{4} x^2y \cos(2v + 4u) - \frac{1}{4} x \cos(2v + 4u) \\ & - \frac{3}{8} x^2y \cos(2v - 2) - \frac{1}{8} x \cos(2v - 2u) \\ & + \frac{3}{4} x^2y + \frac{1}{4} x \end{aligned} \quad (32)$$

which, although seemingly more complex than (31), can be represented computationally very compactly in a list structure.

The Poisson series is not a new representation. E. T. Whittaker [44] has pointed out that those working in celestial mechanics had used this representation in the 19th century. He himself used in the early part of the current century to construct integrals for certain Hamiltonian systems. These integrals he called adelpic integrals.

The significance of the representation of a trigonometric series in the form (30) has been discussed by Fateman [16]. The Poisson series can be successfully represented in computer memory compactly by keeping track of:

1. the type of each term, i.e. whether it is sin or cos,
2. the coefficients of the angular variables,
3. the exponents of the polynomials and
4. the coefficients of the terms.

He further pointed out that this representation is canonical, compact, easy to search and is useful in solving many classes of problems. He employed these ideas in developing the Poisson series subpackage for MACSYMA [30]. It was written in LISP and used list representations to link the term type, angular coefficients, polynomial exponents and term coefficients of each term to each other term. Linked lists are efficient structures for searching for terms, inserting terms and extracting them. All of these operations are needed in algebraically manipulating trigonometric series represented as lists.

Other compact representations of Poisson series for efficient computing have been used in the past. Kovalevsky [28] reviewed some early attempts in Europe to program many of the operations needed to perform symbolic computation in celestial mechanics. In particular, he reviewed the work of Barton [2], whose methods are similar to those used in MACSYMA in that both use linked lists, although Barton used assembly codes to program his algorithms. He represented a Poisson series as a doubly-linked list where the primary chain links the vectors of coefficients of the canonical angular variables. Each of these are in turn linked to the exponents of the first polynomial terms. These then are linked to both their coefficient and to the exponents

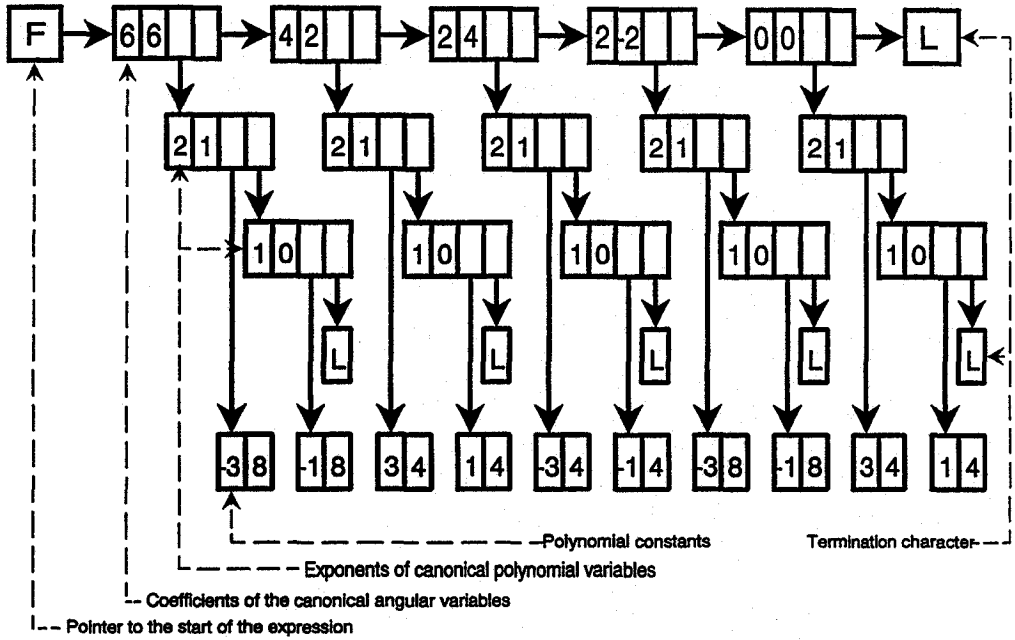


Fig. 1. Barton's doubly linked list storage scheme for the example expression.

of the second polynomial term. The doubly linked list can be continued depending on the length of the series. Figure 1 shows a representation of (32) using Barton's scheme. Note that only the significant constants, coefficients and exponents need to be stored.

Deprit and Rom [10] used Poisson series to develop a high order asymptotic representation of the limit cycle for the van der Pol's equation. It is well known that equation (1) possesses a unique limit cycle for all positive values of the damping coefficient ϵ . In the neighborhood of $\epsilon = 0$ they represented this cycle by a series

$$x(t, \epsilon) = \sum_{n \geq 0} x_n(t) \epsilon^n, \tag{33}$$

the coefficients $x_n(t)$ being periodic functions of t with the minimal period T . The period was represented as a series of the form

$$T = 2\pi \left(1 + \sum_{n \geq 1} T_n \epsilon^n \right). \tag{34}$$

They obtained an asymptotic expansion of the limit cycle up to degree 30 in ϵ . Numerical values were given to ϵ , and the corresponding initial condition and period were evaluated from the series. For ϵ as large as 0.75 the estimates given by the series for the amplitude and the period agreed to 15 decimal places with the correct values. When ϵ reached 1.75 the agreement was still within 10^{-3} .

Melvin [33] used Poisson series to develop the Poincaré-Lindstedt expansion for the van der Pol oscillator in the range $0 \leq \epsilon \leq 1.5$. His approach was to extend his earlier work, Melvin [32], by a numerical construction of the coefficients. Deprit and Schmidt [11] applied a symbolic manipulation package called MAO (for Mechanized Algebraic Operations), developed by Rom [36], to redo the calculations of Melvin and generate the series with coefficients

as exact quotients of relatively prime integers. They developed the limit cycle to order 8 and confirmed Melvin's coefficients were exact to 6 digits with rounding for the last digit.

Several simple trigonometric relations make it feasible to manipulate the Poisson series efficiently. The following identities are used in practice

$$\begin{aligned}\sin A \sin B &= -\frac{1}{2} \cos(A + B) + \frac{1}{2} \cos(A - B) \\ \sin A \cos B &= \frac{1}{2} \sin(A + B) + \frac{1}{2} \sin(A - B) \\ \cos A \cos B &= \frac{1}{2} \cos(A + B) + \frac{1}{2} \cos(A - B).\end{aligned}\tag{35}$$

Another property that will be used subsequently is the following integral

$$\int_0^{2\pi} \int_0^{2\pi} \dots \int_0^{2\pi} \sin(j_1 t_1 + j_2 t_2 \dots j_n t_n) dt_n \dots dt_2 dt_1 = 0\tag{36}$$

with a similar result for cos. In particular this says that an integral of a Poisson series over all its full period is just the leading term with $j_1 = j_2 = \dots = j_n = 0$. The advantage of this property is that an inner product of two trigonometric expressions need not involve an integration. The product of the trigonometric terms can be converted into a Poisson representation and the harmonic terms with nonzero angular coefficients dropped, which is how an inner product of trigonometric terms in MACSYMA can be performed.

5. Applications

Two applications of the Poisson series representation, as an intermediate tool to computing the Galerkin approximation of invariant tori, will be studied. The first application approximates the limit cycle of the classic van der Pol oscillator, which can be considered a one parameter torus. The second application will be to a nonlinearly coupled system of van der Pol oscillators for which a two parameter invariant torus will be constructed.

5.1. VAN DER POL OSCILLATOR

For the classic van der Pol oscillator

$$\ddot{z} - \varepsilon(1 - z^2)\dot{z} + z = 0\tag{37}$$

set

$$\begin{aligned}z &= r \cos \theta. \\ \dot{z} &= r \sin \theta.\end{aligned}\tag{38}$$

Then (37) becomes (see equation (4))

$$\begin{aligned}\dot{\theta} &= 1 + \varepsilon\Theta(\theta, r), \\ \dot{r} &= \varepsilon X(\theta, r),\end{aligned}\tag{39}$$

where

$$\begin{aligned} \Theta(\theta, r) &= (1 - r^2 \cos^2 \theta) \sin \theta \cos \theta, \\ X(\theta, r) &= (1 - r^2 \cos^2 \theta) r \sin^2 \theta. \end{aligned} \tag{40}$$

If $r(\theta)$ is a differentiable parametric representation of a limit cycle of period 2π then by equation (10)

$$\frac{dr}{d\theta}(\theta)(1 + \varepsilon\Theta(\theta, r(\theta))) = \varepsilon X(\theta, r(\theta)). \tag{41}$$

Putting this in the form of equation (11) gives

$$(Nr)(\theta) = \frac{dr}{d\theta}(\theta)(1 + \varepsilon\Theta(\theta, r(\theta))) - \varepsilon X(\theta, r(\theta)). \tag{42}$$

Previous work has shown that only even harmonics are represented in the angular parametric representation of the van der Pol oscillator (see Gilsinn [22]). Thus only even harmonics are assumed in the Galerkin representation of the limit cycle. The essential algorithm used in MACSYMA is relatively straightforward and can be stated as:

1. Initialize the number of even harmonics ℓ and the damping parameter ε .
2. Define the symbols basic representation

$$r_\ell(\theta) = \sum_{\substack{n=0 \\ n(\text{even})}}^{\ell} (a_n \cos(n\theta) + b_n \sin(n\theta)) \tag{43}$$

where the coefficients a_n, b_n are to be determined.

3. In MACSYMA put the complete expansion of the following expression into Poisson form

$$\begin{aligned} (Nr_\ell)(\theta) &= \frac{dr_\ell}{d\theta}(\theta)(1 + \varepsilon((1 - r_\ell(\theta)^2 \cos^2(\theta)) \sin(\theta) \cos(\theta)) \\ &\quad - \varepsilon((1 - r_\ell(\theta)^2 \cos^2(\theta))r_\ell(\theta) \sin^2(\theta)), \end{aligned} \tag{44}$$

where equation (43) has been symbolically substituted.

4. Put each of the basis terms into Poisson form. That is put $1, \cos(n\theta), \sin(n\theta)$, for $n = 2, 4, \dots, \ell$, into Poisson form in MACSYMA.

5. For each of the basis functions form the Poisson products

$$\begin{aligned} &(Nr_\ell)(\theta) \cdot 1, \\ &(Nr_\ell)(\theta) \cdot \cos(n\theta), \\ &(Nr_\ell)(\theta) \cdot \sin(n\theta), \end{aligned} \tag{45}$$

for $n = 2, 4, \dots, \ell$.

6. In MACSYMA there is an operation that can be applied to trim off all harmonic terms of a Poisson series with nonzero angular coefficients. Since (36) holds, apply this trim operation to the products in (45) to get

$$\begin{aligned} &\langle (Nr_\ell)(\theta), 1 \rangle \\ &\langle (Nr_\ell)(\theta), \cos(n\theta) \rangle, \\ &\langle (Nr_\ell)(\theta), \sin(n\theta) \rangle \end{aligned} \tag{46}$$

Table 1. Approximate solution coefficients.

Coeff.	$\varepsilon = 0.5$	$\varepsilon = 1.0$	$\varepsilon = 1.5$
a_0	2.01365	2.05365	2.11428
a_2	-0.03839	-0.14508	-0.2955
b_2	-0.2454	-0.46456	-0.64067
a_4	0.02234	0.07883	0.15199
b_4	0.12123	0.22542	0.31222
a_6	0.01686	0.05226	0.07512
b_6	-0.00622	-0.04375	-0.11723
a_8	-0.01165	-0.03006	-0.03707
b_8	0.00574	0.03403	0.07853
a_{10}	9.2107e-4	0.01209	0.03988
b_{10}	0.00157	0.00654	-1.55835e-4
a_{12}	-0.00123	-0.01142	-0.02715
b_{12}	-0.00133	-0.00195	0.00877
a_{14}	-1.23504e-4	-4.84576e-4	0.00694
b_{14}	1.36739e-4	0.00306	0.01138
a_{16}		-0.00117	-0.00979
b_{16}		-0.00304	-0.00496
a_{18}		-5.47954e-4	-0.00246
b_{18}		2.16835e-4	0.00419
a_{20}			-0.00144
b_{20}			-0.00451
a_{22}			-0.00171
b_{22}			-1.59286e-4
a_{24}			0.00114
b_{24}			-0.00173

for $n = 2, 4, \dots, \ell$. Here the inner product is defined for two functions $r(\theta)$ and $g(\theta)$, both periodic with period 2π in all components of θ , as

$$\langle r, g \rangle = \frac{1}{2\pi} \int_0^{2\pi} r(\theta)g(\theta) d\theta. \quad (47)$$

The end result of (28) is to produce $\ell + 1$ equations in $\ell + 1$ unknown parameters.

7. These nonlinear equations are solved in MACSYMA by Newton's method. The only limitation on the entire process is the number of equations that can be held in memory.

The coefficients of the even terms in the expansion of the parameterized form of the limit cycle are given in Table 1 and are those used in equation (43). The expansion coefficients are shown for the case of $\varepsilon = 0.5, 1.0$ and 1.5 . Further cases could have been considered but they would not have added further information to the fact that the Galerkin approximations of sufficient length appear to converge adequately. All expansions were performed on a 486/33 PC with 32M Bytes of memory.

Table 2. Maximum error between the full system and phase equation on the limit cycle.

	$\varepsilon = 0.5$	$\varepsilon = 1.0$	$\varepsilon = 1.5$
θ	$3.20435e-4$	$7.711411e-3$	0.131990
r	$5.25951e-4$	$8.93307e-3$	0.212730

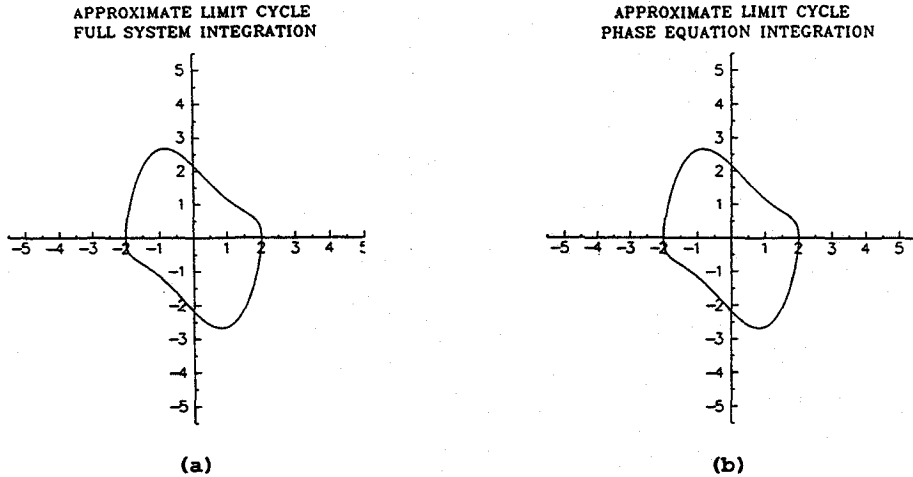


Fig. 2. Trajectories on the limit cycle: (a) full system, (b) phase equation only ($\varepsilon = 1.0$). Initial conditions on the approximate limit cycle. Integration step size 0.05, number of steps = 500.

The error trends were then computed between the numerically integrated angle-radial equations, equation (39), and the approximate system, given by

$$\begin{aligned} \dot{\theta} &= 1 + \varepsilon\Theta(\theta, r_\ell(\theta)), \\ r &= r_\ell(\theta). \end{aligned} \tag{48}$$

This system represents the integration of the phase equation on the approximate torus. In all case studies for both the single and coupled oscillators Gear's method (see Gear [20]) was used. Equations (39) and (48) were integrated with 500 steps of length 0.05. The coefficients for $r_\ell(\theta)$ in (48) for the case $\varepsilon = 0.5$ are the 15 coefficients in the column under $\varepsilon = 0.5$ in Table 1. The coefficients for the other two cases are in their respective columns. The maximum absolute error between (39) and (48) are shown in Table 2. For the given number of simulation steps the maximum absolute errors in this case show an excellent fit. In all three cases plots of the limit cycles for the integration of the full and approximate system are indistinguishable. Figure 2 shows the results for $\varepsilon = 1.0$.

As another measure of the quality of the approximation the Fourier spectrum of the phase and radial solutions for (39) and the phase and radial solutions for (48) were computed. The spectra are nearly identical and are graphically demonstrated in Figure 4. Table 3 shows that for $\varepsilon = 0.5$ the dominant angular frequencies ($\omega = 2\pi f$, f in Hertz) very nearly duplicate the ideal angular frequencies shown in column 1. The angular frequencies in Table 3 are computed from the time dependent solutions of (48) with linear trends subtracted out. Although these seven

Table 3. Dominant frequency response of the phase equation on the limit cycle.

Ideal ω	$\varepsilon = 0.5$		$\varepsilon = 1.0$		$\varepsilon = 1.5$	
	θ	r	θ	r	θ	r
2	2.011	2.011	2.011	1.759	1.759	1.759
4	4.021	4.021	3.770	3.770	3.519	3.519
6	6.032	5.781	5.781	5.529	5.278	5.278
8	8.042	7.791	7.791	7.540	7.037	7.037
10	10.05	9.802	9.299	9.550	8.796	8.796
12	11.81	11.81	11.56	11.31	10.56	10.56
14	13.82	13.82	13.07	13.07	12.32	12.32
16	-	-	15.08	15.08	14.07	14.07
18	-	-	-	16.84	15.83	15.83
20	-	-	-	-	17.59	17.59
22	-	-	-	-	19.35	19.35
24	-	-	-	-	21.36	21.36

Table 4. Dominant frequency response of the full system on the limit cycle.

Ideal ω	$\varepsilon = 0.5$		$\varepsilon = 1.0$		$\varepsilon = 1.5$	
	θ	r	θ	r	θ	r
2	2.011	2.011	2.011	1.759	1.759	1.759
4	4.021	4.021	3.770	3.770	3.519	3.519
6	6.032	5.781	5.781	5.529	5.278	5.278
8	8.042	7.791	7.791	7.540	7.037	7.037
10	10.05	9.802	-	9.550	8.796	8.796
12	11.81	11.81	11.56	11.56	10.56	10.56
14	13.82	13.82	13.07	13.07	12.32	12.32
16	-	-	15.08	15.08	14.07	14.07
18	-	-	17.09	-	15.83	15.83
20	-	-	-	-	17.59	17.59
22	-	-	-	-	19.60	19.60
24	-	-	-	-	21.36	21.36

even frequencies are somewhat expected considering the assumed approximate parametric expansion of the limit cycle, these frequencies track those of the full system integration as shown in Table 4. Note that in these and other frequency tables in this report some of the entries are blank. This means that those frequencies were too small to detect or were small relative to nearby frequencies, such as side lobes.

Observations similar to the above can be made about the cases $\varepsilon = 1.0$, $\varepsilon = 1.5$. Notice however that as the numerical accuracy decreases in Table 2 the frequencies in Table 3 show shifts from the expected angular frequencies. Plots in Figure 3 show that for the case $\varepsilon = 1.0$ there are periodic components to both angular and radial errors as well as a definite increasing trend. Extending the number of basis elements used reduced the error range for the same time

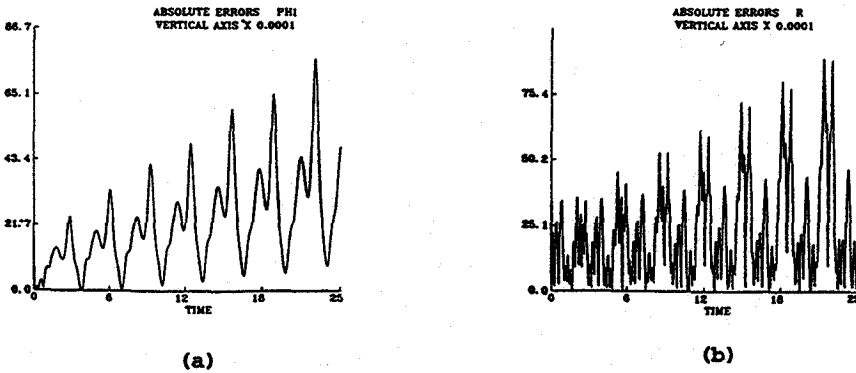


Fig. 3. Absolute errors between integrating the full system and the phase equation on the limit cycle. (a) shows the phase differences and (b) shows the radial differences. Initial conditions are as in Figure 2.

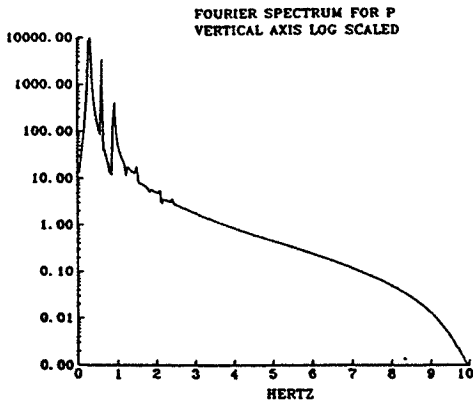
interval, but the error trends still increase as time increases. For the case $\varepsilon = 0.5$ the linear trend was not dominant but it was for the case $\varepsilon = 1.5$. These trends can be explained in terms of the integration algorithm used and will be discussed in a separate section below.

The size and complexity of the MACSYMA calculations can be illustrated by the number of terms in the equations that must be solved to generate the Galerkin coefficients. The average number of terms in the variational equations for the case $\varepsilon = 0.5$ is 267. In the $\varepsilon = 1.0$ case there are 19 equations and 19 unknowns. However, the average number of terms in the variational equations for the case $\varepsilon = 1.0$ is 478 and the number for the case $\varepsilon = 1.5$ could not be computed along with solving the equations without 'hanging' the system.

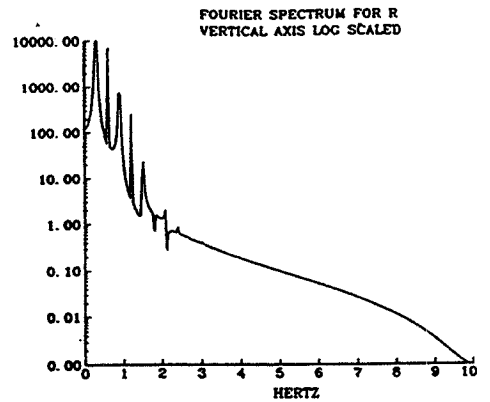
For a given $\varepsilon > 0$ and a given maximum integration time it appears to be possible to select the number of terms in the Galerkin approximation to maintain errors within prescribed bounds. However, the tighter the error specification the number of terms required begins to grow rapidly. The memory available to MACSYMA of course limits these expansions. An attempt was made by the author on the 486 PC to extend the basis set for the case $\varepsilon = 1.5$ in order to reduce the error. However, MACSYMA, although generating the variation equations, could not perform the Newton approximation and simply 'hung'. It was clear that memory limitations had been reached. For the given selection of basis terms for each of the ε values the maximum absolute errors increase with increasing ε . Further reduction in absolute errors would require increasing the basis set, thus increasing the harmonics in the approximation. The ability to do this clearly depends on usable memory available which also depends on how the operating system accesses memory.

Again, as a final test on the quality of the approximation the power spectra of the angular and radial equations for the integration of the angular-radial system for the two cases $\varepsilon = 1.0, 1.5$ are given in Tables 3 and 4. A perusal of these two tables clearly shows that the Galerkin method does as well as numerical methods in generating frequencies.

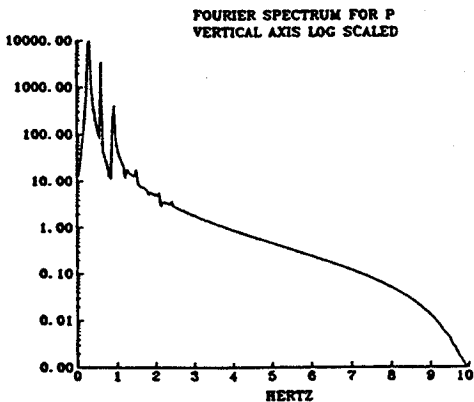
Table 3 reflects Table 2. It shows that the angular frequencies nearly match the expected or ideal frequencies used in the approximations provided the basis set is sufficiently extensive. For $\varepsilon = 0.5$ selecting a basis set of seven even harmonics from 2 to 14 gave a good approximation for the integration period selected. For $\varepsilon = 1.0$ only four computed angular frequencies round to the ideal and for $\varepsilon = 1.5$ only two properly round. The errors shown in Table 2 mirror these approximations. This suggests the result that given an integration period and an ε there exists a basis set of even harmonics that produces an absolute integration error of less than a



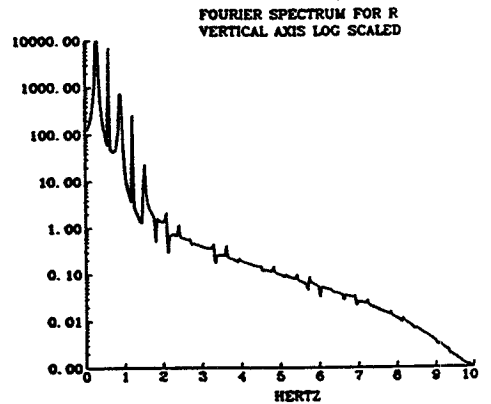
(a)



(b)



(c)



(d)

Fig. 4. Spectral plots of the amplitudes of the phase and radial equations for the full system, (a) phase, (b) radial, and the approximate system, (c) phase, (d) radial. Initial conditions as in Figure 2.

prescribed amount. The relationship of the approximation obtained and the actual frequencies produced is a question for further research.

As a note of interest, the Galerkin method as discussed in this paper holds a close affinity to the Method of Harmonic Balance as described, for instance, in Nayfeh and Mook [34]. Galerkin's method, however, can be implemented more efficiently in MACSYMA. Both methods seek to generate a set of algebraic equations that must be solved to compute the coefficients of the assumed approximate solution, in this case equation (43). In fact all of the steps of the previous MACSYMA algorithm would be the same for harmonic balance except for numbers 4, 5 and 6. At this point, instead of being able to project out the variational

equations by a simple trimming of all harmonics in the Poisson series, one would have to write an algorithm in MACSYMA to compare all of the harmonics produced by expanding (44) with those in (43) in order to identify the terms to drop from the expansion of (44). This is not a straightforward process, since each term would have to be syntactically parsed to form the leading polynomial and the harmonic portion before the harmonic portion could be compared with those in (43). Thus it is clear that, although they are intimately related, Galerkin's projection steps lend themselves to more efficient programming than harmonic balance in MACSYMA. These comments also apply to the assumed expansions for the torus as described in the next section. For an example of the steps required to apply a symbolic manipulation program to the solution of a nonlinear oscillation problem by harmonic balance see Wang and Huseyin [43]. They provide a source code example from the language MAPLE.

5.2. COUPLED VAN DER POL OSCILLATORS

The example considered in this section is the system

$$\begin{aligned} \ddot{z}_1 + \omega_1^2 z_1 &= \varepsilon(1 - z_1^2 - az_2^2)\dot{z}_1, \\ \ddot{z}_2 + \omega_2^2 z_2 &= \varepsilon(1 - \alpha z_1^2 - z_2^2)\dot{z}_2. \end{aligned} \tag{49}$$

This system has also been studied by the author in [22] where a perturbation series formula was developed for an invariant torus in the case of small $\varepsilon > 0$. The first step in developing a representation for an invariant tori for (49) was to reduce it to the form (4). This was done by introducing the polar type coordinate

$$\begin{aligned} z_1 &= x_1^{1/2} \sin(\omega_1 \theta_1), \\ \dot{z}_1 &= \omega_1 x_1^{1/2} \cos(\omega_1 \theta_1), \\ z_2 &= x_2^{1/2} \sin(\omega_2 \theta_2), \\ \dot{z}_2 &= \omega_2 x_2^{1/2} \cos(\omega_2 \theta_2). \end{aligned} \tag{50}$$

Then (49) becomes (4) with

$$\begin{aligned} \Theta_1(\theta, x) &= -\left(\frac{1}{\omega_1}\right) (\sin(\omega_1 \theta_1) \cos(\omega_1 \theta_1) - x_1 \sin^3(\omega_1 \theta_1) \cos(\omega_1 \theta_1) \\ &\quad - ax_2 \sin(\omega_1 \theta_1) \cos(\omega_1 \theta_1) \sin^2(\omega_2 \theta_2)), \\ \Theta_2(\theta, x) &= -\left(\frac{1}{\omega_2}\right) (\sin(\omega_2 \theta_2) \cos(\omega_2 \theta_2) - \alpha x_1 \sin^2(\omega_1 \theta_1) \sin(\omega_2 \theta_2) \cos(\omega_2 \theta_2) \\ &\quad - x_2 \sin^3(\omega_2 \theta_2) \cos(\omega_2 \theta_2)), \\ X_1(\theta, x) &= 2x_1(\cos^2(\omega_1 \theta_1) - x_1 \sin^2(\omega_1 \theta_1) \cos^2(\omega_1 \theta_1) - ax_2 \cos^2(\omega_1 \theta_1) \sin^2(\omega_2 \theta_2)), \\ X_2(\theta, x) &= 2x_2(\cos^2(\omega_2 \theta_2) - \alpha x_1 \sin^2(\omega_1 \theta_1) \cos^2(\omega_2 \theta_2) \\ &\quad - x_2 \sin^2(\omega_2 \theta_2) \cos^2(\omega_2 \theta_2)). \end{aligned} \tag{51}$$

From the form of (51) it seemed appropriate to look for $S(\theta)$ as multiple Fourier series with period $\frac{2\pi}{\omega_1}$ in θ_1 , $\frac{2\pi}{\omega_2}$ in θ_2 . For the case of a real valued double Fourier series, if it has continuous

and bounded second partial derivatives then the double Fourier series converges absolutely and uniformly. For the current problem $S(\theta)$ will be taken as a vector of two components since x is a two dimensional vector. The N -th partial sum will be designated as

$$S_N(\theta) = \begin{pmatrix} S_N^{(1)}(\theta) \\ S_N^{(2)}(\theta) \end{pmatrix} \tag{52}$$

where

$$S_N^{(i)}(\theta) = \sum_{n=0}^N \sum_{m=0}^N (a_{nm}^{(i)} \cos(\omega_1 n \theta_1) \cos(\omega_2 m \theta_2) + b_{nm}^{(i)} \cos(\omega_1 n \theta_1) \sin(\omega_2 m \theta_2) + c_{nm}^{(i)} \sin(\omega_1 n \theta_1) \cos(\omega_2 m \theta_2) + d_{nm}^{(i)} \sin(\omega_1 n \theta_1) \sin(\omega_2 m \theta_2)) \tag{53}$$

and the coefficients were determined for $i = 1, 2$. Certain of the coefficients were understood as 0. For those terms, where $n = 0$, or $m = 0$, the sin components were 0.

In terms of components (42) was written as two separate partial differential equations

$$\begin{aligned} (NS^{(1)})(\theta) &= \frac{\partial S^{(1)}}{\partial \theta_1} + \frac{\partial S^{(1)}}{\partial \theta_2} + \varepsilon \frac{\partial S^{(1)}}{\partial \theta_1} \Theta_1(\theta, S(\theta)) \\ &\quad + \varepsilon \frac{\partial S^{(1)}}{\partial \theta_2} \Theta_2(\theta, S(\theta)) - \varepsilon X_1(\theta, S(\theta)) = 0 \\ (NS^{(2)})(\theta) &= \frac{\partial S^{(2)}}{\partial \theta_1} + \frac{\partial S^{(2)}}{\partial \theta_2} + \varepsilon \frac{\partial S^{(2)}}{\partial \theta_1} \Theta_1(\theta, S(\theta)) \\ &\quad + \varepsilon \frac{\partial S^{(2)}}{\partial \theta_2} \Theta_2(\theta, S(\theta)) - \varepsilon X_2(\theta, S(\theta)) = 0. \end{aligned} \tag{54}$$

The variational equations that were solved were given by

$$\begin{aligned} \langle (NS^{(i)})(\theta), \cos(\omega_1 n \theta_1) \cos(\omega_2 m \theta_2) \rangle &= 0, \\ \langle (NS^{(i)})(\theta), \cos(\omega_1 n \theta_1) \sin(\omega_2 m \theta_2) \rangle &= 0, \\ \langle (NS^{(i)})(\theta), \sin(\omega_1 n \theta_1) \cos(\omega_2 m \theta_2) \rangle &= 0, \\ \langle (NS^{(i)})(\theta), \sin(\omega_1 n \theta_1) \sin(\omega_2 m \theta_2) \rangle &= 0, \end{aligned} \tag{55}$$

for $i = 1, 2$, where the inner product is defined by

$$\langle r, g \rangle = \frac{\omega_1 \omega_2}{4\pi^2} \int_0^{2\pi/\omega_1} \int_0^{2\pi/\omega_2} r(\theta_1, \theta_2) g(\theta_1, \theta_2) d\theta_2 d\theta_1. \tag{56}$$

The first step in approximating invariant tori was to locate potential candidates. To do this N was set to 0 in (53). From (54), (55) and (56) only two equations had to be solved,

$$\begin{aligned} a_{00}^{(1)} \left(1 - \frac{a_{00}^{(1)}}{4} - a \frac{a_{00}^{(2)}}{2} \right) &= 0, \\ a_{00}^{(2)} \left(1 - \alpha \frac{a_{00}^{(1)}}{2} - \frac{a_{00}^{(2)}}{4} \right) &= 0. \end{aligned} \tag{57}$$

These were, incidentally, the same two equations that had to be solved to locate potential invariant tori using the average technique developed by Gilsinn [22]. There were four solutions for (57), given by

$$\begin{aligned}
 1. \quad & a_{00}^{(1)} = a_{00}^{(2)} = 0, \\
 2. \quad & a_{00}^{(1)} = 0, \quad a_{00}^{(2)} = 4, \\
 3. \quad & a_{00}^{(1)} = 4, \quad a_{00}^{(2)} = 0, \\
 4. \quad & a_{00}^{(1)} = \frac{4 - 8a}{1 - 4a\alpha}, \quad a_{00}^{(2)} = \frac{4 - 8\alpha}{1 - 4a\alpha}.
 \end{aligned} \tag{58}$$

The first solution represented the trivial original solution. The next two represented separate limit cycles and were the first order approximations to the radii of the limit cycles. Note that the radial values are 4 since the transformations in (50) have an exponent of $\frac{1}{2}$ as a device to simplify the resulting equations. The last solution represented the invariant torus. As shown in Gilsinn [22] an appropriate region of asymptotic stability of the torus was determined by the parameter region $0 < a < \frac{1}{2}, 0 < \alpha < \frac{1}{2}$. To be more specific the following parameters remained fixed for this case study:

$$\begin{aligned}
 a &= 0.20, \\
 \alpha &= 0.40, \\
 \omega_1 &= 1.0, \\
 \omega_2 &= 1.414.
 \end{aligned} \tag{59}$$

From (58) the first approximation to the radii were $a_{00}^{(1)} = 3.53, a_{00}^{(2)} = 1.18$. Tables 5 and 6 list the coefficients computed by both the averaging based approximation developed by the author in [22] for $\epsilon = 0.05$ and the coefficients computed by the Galerkin approximation for $\epsilon = 0.05, 0.5, 1.0$. As can be seen from the tables the coefficients from the averaging and those from the Galerkin approximation for $\epsilon = 0.05$ were very close. The averaging method however did not generate coefficients for terms of the order of 1×10^{-3} or smaller.

The symbolic algorithm for computing these coefficients is similar to the algorithm used to compute the limit cycle of the van der Pol oscillator. Before beginning however the following substitutions were made to transform (54) into a form that could be expanded as a Poisson series:

$$\begin{aligned}
 x &= \omega_1 \theta_1, \\
 y &= \omega_2 \theta_2.
 \end{aligned} \tag{60}$$

The MACSYMA algorithm then became:

1. Initialize the number of even harmonics ℓ and the damping parameter ϵ .
2. Define the two symbolic basis representations:

$$s1_\ell(x, y) = \sum_{\substack{n=0 \\ n(\text{even})}}^{\ell} \sum_{\substack{m=0 \\ m(\text{even})}}^{\ell} (a_{1nm} \cos(nx) \cos(my) + b_{1nm} \cos(nx) \sin(my))$$

Table 5. Coefficients for the approximate torus.

Coeff.	Averaged $\epsilon = 0.05$	Galerkin		
		$\epsilon = 0.05$	$\epsilon = 0.5$	$\epsilon = 1.0$
a_{100}	3.52941	3.52981	3.57764	3.74297
a_{120}		0.00161	0.14848	0.50194
c_{120}	0.07785	0.07783	0.76096	1.46385
a_{140}		4.8305e-4	0.0508	0.21725
c_{140}	0.03893	0.03893	0.39509	0.82167
a_{102}		-1.15736e-5	0.01108	0.09261
b_{102}	0.007341	0.00737	0.09197	0.20859
a_{104}		-3.9817e-5	-0.00234	-0.00734
b_{104}		2.0644e-6	8.43295e-4	-7.16953e-4
a_{122}		0.00126	0.09832	0.27036
b_{122}	0.01469	0.01461	0.09642	0.09347
c_{122}	-0.01039	-0.01029	-0.03782	-0.06894
d_{122}		0.00154	0.11586	0.29067
a_{124}		-8.03012e-5	-0.01197	-0.05671
b_{124}		-4.22521e-6	-8.06277e-4	0.01969
c_{124}		3.76436e-6	-6.75525e-4	-0.01863
d_{124}		-5.30407e-5	-0.00864	-0.04021
a_{142}		-3.86687e-4	-0.02074	-0.00394
b_{142}		9.9227e-6	0.00746	0.04247
c_{142}		-2.8437e-6	-0.00188	-0.03848
d_{142}		-1.75136e-4	0.00167	0.07459
a_{144}		-1.59375e-4	-0.00844	0.00469
b_{144}		1.72939e-5	0.0128	0.05859
c_{144}		-1.80894e-5	-0.01319	-0.05961
d_{144}		-1.50128e-4	-0.00703	0.01202

$$\begin{aligned}
 &+ c_{1nm} \sin(nx) \cos(my) + d_{1nm} \sin(nx) \sin(my)), \\
 s2_\ell(x, y) = &\sum_{\substack{n=0 \\ n(\text{even})}}^{\ell} \sum_{\substack{m=0 \\ m(\text{even})}}^{\ell} (a_{2nm} \cos(nx) \cos(my) + b_{2nm} \cos(nx) \sin(my) \\
 &+ c_{2nm} \sin(nx) \cos(my) + d_{2nm} \sin(nx) \sin(my)). \tag{61}
 \end{aligned}$$

3. Put $\epsilon\Theta_1, \epsilon\Theta_2, \epsilon X_1, \epsilon X_2$ into Poisson representation after inserting $s1_\ell$, and $s2_\ell$.
4. Put $s1_\ell$ and $s2_\ell$ into Poisson form.
5. Compute the derivatives $\omega_1 \frac{\partial s1_\ell}{\partial x}, \omega_2 \frac{\partial s2_\ell}{\partial y}, \omega_2 \frac{\partial s1_\ell}{\partial y}, \omega_1 \frac{\partial s2_\ell}{\partial x}$ in Poisson form.
6. By using Poisson summation form the expressions for $(NS^{(1)})(x, y)$ and $(NS^{(2)})(x, y)$ from (54).
7. For $n, m = 0, \dots, \ell$ put all of the basis elements

$$\begin{aligned}
 &\cos(nx) \cos(my) \\
 &\cos(nx) \sin(my)
 \end{aligned}$$

Table 6. Coefficients for the approximate torus.

Coeff.	Averaged $\epsilon = 0.05$	Galerkin		
		$\epsilon = 0.05$	$\epsilon = 0.5$	$\epsilon = 1.0$
a_{200}	1.17647	1.17652	1.16989	1.07185
a_{220}		3.88936e-4	0.03478	0.09534
c_{220}	0.02076	0.02075	0.19404	0.31232
a_{240}		3.82244e-5	0.0043	0.01902
c_{240}		3.7533e-6	0.00271	0.01006
a_{202}		-3.87425e-4	-0.0301	-0.07748
b_{202}	0.006118	0.00614	0.07512	0.16681
a_{204}		-7.5554e-5	-0.00427	-0.00585
b_{204}	0.003059	0.00307	0.03565	0.07392
a_{222}		5.78693e-4	0.04187	0.06161
b_{222}	0.02937	0.02934	0.26475	0.44625
c_{222}	-0.02077	-0.02075	-0.18939	-0.33731
d_{222}		2.09716e-4	0.01118	-0.02793
a_{224}		-9.5337e-6	-0.00624	-0.04413
b_{224}		-1.06561e-5	0.00668	-0.03141
c_{224}		1.11702e-5	0.00833	0.04891
d_{224}		1.15034e-4	0.00688	0.71993e-5
a_{242}		-2.43808e-4	-0.02108	-0.06231
b_{242}		3.19611e-6	0.00423	0.03415
c_{242}		-1.33117e-7	-0.0015	-0.02107
d_{242}		-1.83154e-4	-0.01605	-0.05281
a_{244}		-3.20202e-4	-0.02741	-0.10108
b_{244}		9.20099e-6	0.00584	0.01424
c_{244}		-8.41689e-6	-0.00504	-0.00895
d_{244}		-3.01856e-4	-0.02558	-0.09529

$$\begin{aligned} &\sin(nx) \cos(my) \\ &\sin(nx) \sin(my) \end{aligned} \tag{62}$$

into Poisson form.

8. For $i = 1, 2$ and $n, m = 0, \dots, \ell$, using Poisson multiplication, put the expressions

$$\begin{aligned} &(NS^{(i)})(x, y) \cos(nx) \cos(my) \\ &(NS^{(i)})(x, y) \cos(nx) \sin(my) \\ &(NS^{(i)})(x, y) \sin(nx) \cos(my) \\ &(NS^{(i)})(x, y) \sin(nx) \sin(my) \end{aligned} \tag{63}$$

into Poisson form.

9. Compute the inner products (55) by trimming off all harmonic terms with $n, m = 1, \dots, \ell$. This gives the algebraic expressions for (55).

10. Solve these by Newton's method.

Table 7. Maximum error between the full system and phase equations on the torus.

	$\varepsilon = 0.05$	$\varepsilon = 0.5$	$\varepsilon = 1.0$
θ_1	9.186e-3	0.918	11.179
θ_2	2.502e-3	0.131	1.276
x_1	2.579e-3	1.953	5.503
x_2	8.160e-4	0.502	1.458

Tables 5 and 6 give the coefficients for the even harmonic terms up to 4. Each harmonic included in the assumed expansion increased the number of unknowns and resulting equations by 16. Each of the variational equations had several hundred terms. Because of the limitations of the PC only even harmonic terms up to 4 could be used. A workstation version of MACSYMA was not available to the author. It, no doubt, could have extended these limits. The results discussed below however indicate strongly that the Galerkin method, used in conjunction with the Poisson series representation, is an adequate technique for approximating invariant tori for systems with large damping parameters.

Table 7 shows the results of integrating the full system (4), using (51), and the approximate phase equations on the torus given by

$$\begin{aligned}\dot{\theta} &= \mathbf{d} + \varepsilon \Theta(\theta, \mathbf{S}_N(\theta)), \\ \mathbf{x} &= \mathbf{S}_N(\theta).\end{aligned}\tag{64}$$

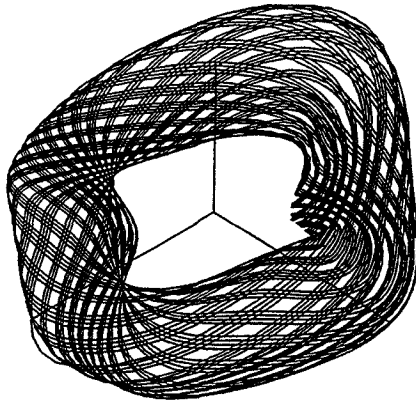
The integration step size was 0.1 and the number of integration steps was 4000. The table gives the absolute errors between the phase and radial results for both the full and approximate systems.

For the case $\varepsilon = 0.05$ the phase difference errors showed increases whereas the radial differences oscillate around a mean. In both cases the absolute errors are small. The main peaks of the Fourier spectra of the time integration of (4) and (64) respectively for this case are shown in Table 8. These results are also very comparable to those given in Gilsinn [22]. This suggests that, at least for small ε , the averaging and Galerkin methods are consistent.

In Table 8, column 1 represents the linear combinations of the angular frequencies in radians per second, whereas the other column are given in Hertz. For example, from the first row, using (59), $2\omega_2 - \omega_1 = 0.828$ radians per second. After dividing by 2π this is given approximately by 0.132 Hz, which is shown in column 2. The other three columns are the frequencies in Hertz computed by integrating (64) using the Galerkin coefficients for $\varepsilon = 0.05$ in Tables 5 and 6. These angular frequency combinations indicate the aperiodicity of the solutions on the torus.

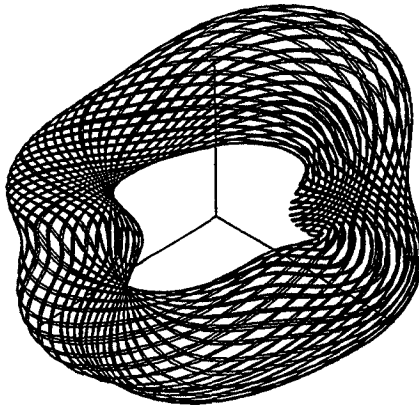
Figure 5 shows the full and approximate system integration for the case $\varepsilon = 0.5$. Initial conditions for both integrations were taken on the approximate torus. The integration step size and number were the same as in the case $\varepsilon = 0.05$. Figure 6 shows the error trends. There is an increasing trend with oscillations about it for both the angular and radial solutions. An explanation for this can be found as indicated earlier in the numerical scheme used to integrate the differential equations and will be discussed below.

APPROXIMATE TORUS
FULL SYSTEM INTEGRATION



(a)

APPROXIMATE TORUS
PHASE EQUATION INTEGRATION

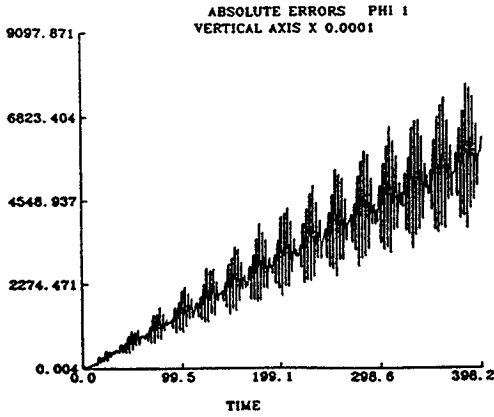


(b)

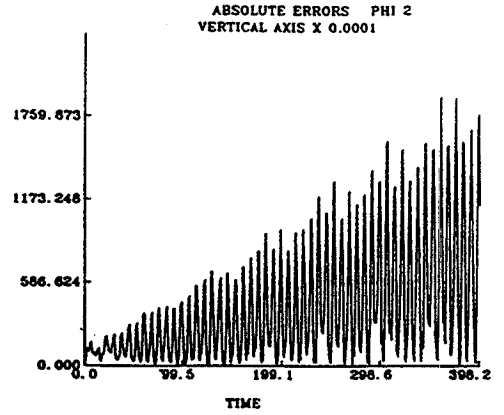
Fig. 5. Trajectories on the torus: (a) full system, (b) phase equations only ($\varepsilon = 0.5$). Initial conditions on the approximate torus. Integration step size 0.1, number of steps = 4000.

Figures 7 and 8 show the spectral plots from integrating the full system in the form (4), using (51), and the approximate system (64) with coefficients taken from Tables 5 and 6 in the Galerkin columns for $\varepsilon = 0.5$. Tables 9 and 10 show the frequencies in Hertz that compare with the theoretical angular frequencies given in column 1. For this value of ε the frequencies in these two tables are quite similar.

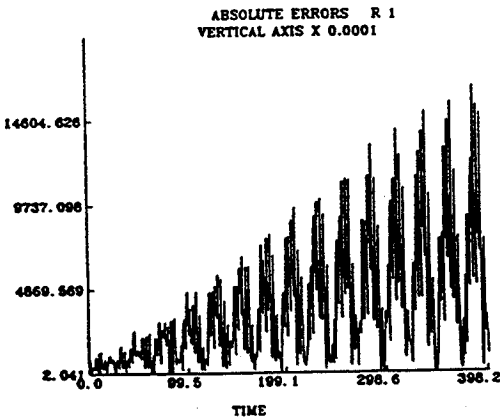
The error trends between the full and approximate system integration for $\varepsilon = 1.0$ on the torus show similar trends to those for $\varepsilon = 0.5$. The errors are large since only harmonics 2 and 4 are used in the approximate solutions. The PC used was not able to handle a larger expansion. These larger errors are reflected in the frequency Tables 11 and 12 where it is clear that there are definite frequency shifts in the approximate solutions.



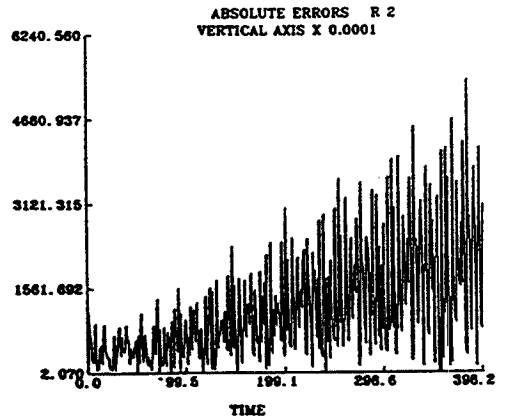
(a)



(b)



(c)



(d)

Fig. 6. Absolute errors between integrating the full system and the phase equations on the torus. (a) and (b) show the phase differences where (c) and (d) show the radial differences. Initial conditions as in Figure 5.

6. MACSYMA Program for the Torus

In this section the MACSYMA program for the simple case of one even harmonic is given in order to demonstrate how the Poisson representation was used to perform efficient intermediate representations of the trigonometric terms. The program syntax is not particularly difficult to understand. Lines beginning with `/*` and ending with `*/` are comments. Lines terminating with `$` suppress any output, while those ending with `;` produce an output after execution. The colon `;` is an assignment operator. Array elements are identified by square brackets after

Table 8. Major frequency responses in Hertz after the integration of the full system and phase equations starting on the approximate torus ($\epsilon = 0.05$).

$\epsilon = 0.05$					
Full system integration					
Ang. freq.	Theory	θ_1	θ_2	X_1	X_2
$2\omega_2 - 2\omega_1$	0.132	0.132	0.132	0.132	0.132
$2\omega_1$	0.318	0.318	0.318	0.318	0.318
$2\omega_2$	0.450	0.450	0.450	0.450	0.450
$4\omega_1$	0.637	0.637	-	0.637	0.637
$2\omega_2 + 2\omega_1$	0.768	0.767	0.767	0.767	0.767
$4\omega_2$	0.900	-	0.900	-	0.900
$6\omega_1$	0.955	0.955	-	0.955	-
-	-	-	-	-	1.087
$4\omega_2 + 2\omega_1$	1.2185	-	-	-	1.2175
$8\omega_1$	1.273	-	-	-	-
Integration of phase equations on the approximate torus					
$2\omega_2 - 2\omega_1$	0.132	0.133	0.133	0.133	0.133
$2\omega_1$	0.318	0.318	0.318	0.318	0.318
$2\omega_2$	0.450	0.450	0.450	0.450	0.450
$4\omega_1$	0.637	0.637	0.637	0.637	0.637
$2\omega_2 + 2\omega_1$	0.767	0.767	0.767	0.767	0.767
$4\omega_2$	0.900	-	0.900	-	0.900
$6\omega_1$	0.955	0.955	-	0.955	0.955
-	-	-	-	-	1.087
$4\omega_2 + 2\omega_1$	1.2185	-	-	-	1.2175
$8\omega_1$	1.273	-	-	1.273	-

the array variable name, e.g. $a[1,2,3]$ for the element (1,2,3) of array a . Algebraic operations in expressions use the standard symbols, except that exponentiation is designated by \wedge . For loops with the step option are straightforward. A more detailed explanation is given in the MACSYMA reference manual [30].

```

/* Load the Poisson package and set the harmonic limits for intermediate expressions */
load(pois2)$
poislim:60$
/* Set the maximum basis harmonics for this run and expand the assumed solutions */
/* Algorithm Step: 1 */
1:2$
/* Algorithm Step: 2 */
s1:0$
s2:0$
/* For loops are similar to FORTRAN or BASIC loops */

```

```

for n:0 step 2 thru 1 do
  for m:0 step 2 thru 1 do
    (s1:s1 + a[1,n,m]*cos(n*x)*cos(m*y)
      + b[1,n,m]*cos(n*x)*sin(m*y)
      + c[1,n,m]*sin(n*x)*cos(m*y)
      + d[1,n,m]*sin(n*x)*sin(m*y),
    s2:s2 + a[2,n,m]*cos(n*x)*cos(m*y)
      + b[2,n,m]*cos(n*x)*sin(m*y)
      + c[2,n,m]*sin(n*x)*cos(m*y)
      + d[2,n,m]*sin(n*x)*sin(m*y))$
/* Set up the first order partial differential equations */
/* Algorithm Step: 3 */
/* To do this, first evaluate theta(1), theta(2), x(1), x(2) multiplied by eps. See (33) and (36). */
/* Evaluate them for the fixed parameters then put them in Poisson form */
exp1:-(eps/mu1)*(sin(x)*cos(x) - s1*sin(x)^3*cos(x)
  -ac*s2*sin(x)*cos(x)*sin(y)^2)$
exp1:subst([eps=0.5,ac=0.20,mu1=1.0],exp1)$
et1:intopois(exp1)$
exp2:-(eps/mu2)*(sin(y)*cos(y) - alpha*s1*sin(x)^2*sin(y)*cos(y)
  -s2*sin(y)^3*cos(y))$
exp2:subst([eps=0.5,alpha=0.40,mu2=1.414],exp2)$
et2:intopois(exp2)$
exp3:-eps^2*s1*(cos(x)^2 - s1*sin(x)^2*cos(x)^2
  -ac*s2*cos(x)^2*sin(y)^2)$
exp3:subst([eps=0.5,ac=0.20],exp3)$
emx1:intopois(exp3)$
exp4:-eps^2*s2*(cos(y)^2 - alpha*s1*sin(x)^2*cos(y)^2
  -s2*sin(y)^2*cos(y)^2)$
exp4:subst([eps=0.5,alpha=0.40],exp4)$
emx2:intopois(exp4)$
/* Algorithm Step: 4 */
/* Introduce the frequency parameters and put s1 and s2 into Poisson form */
t[1,1]:subst([mu1=1.0],mu1*s1);
mu1s1:intopois(t[1,1])$
t[2,1]:subst([m2=1.414],mu2*s1);
mu2s1:intopois(t[2,1])$
t[1,2]:subst([mu1=1.0],mu1*s2);
mu1s2:intopois(t[1,2])$
t[2,2]:subst([mu2=1.414],mu2*s2);
mu2s2:intopois(t[2,2])$
/* Algorithm Step: 5 */
/* Get Partial Derivatives */
dmu1s1dx:poisdiff(mu1s1,x)$
dmu2s1dy:poisdiff(mu2s1,y)$
dmu1s2dx:poisdiff(mu1s2,x)$
dmu2s2dy:poisdiff(mu2s2,y)$
/* Algorithm Step: 6 */

```

```

/* First PDE */
ns[1]:poisplus(dmu1s1dx,dmu2s1dy)$
temp:poistimes(dmu1s1dx,et1)$
ns[1]:poisplus(ns[1],temp)$
temp:poistimes(dmu2s1dy,et2)$
ns[1]:poisplus(ns[1],temp)$
ns[1]:poisplus(ns[1],emx1)$
/* Second PDE */
ns[2]:poisplus(dmu1s2dx,dmu2s2dy)$
temp:poistimes(dmu1s2dx,et1)$
ns[2]:poisplus(ns[2],temp)$
temp:poistimes(dmu2s2dy,et2)$
ns[2]:poisplus(ns[2],temp)$
ns[2]:poisplus(ns[2],emx2)$
/* Algorithm Step: 7 */
/* Put the basis functions into Poisson form */
basis[1]:intopois(1)$
k:2$
for n:2 step 2 thru 1 do
  (basis[k]:intopois(cos(n*x)), k:k+1)$
for n:2 step 2 thru 1 do
  (basis[k]:intopois(sin(n*x)), k:k+1)$
for m:2 step 2 thru 1 do
  (basis[k]:intopois(cos(m*y)), k:k+1)$
for m:2 step 2 thru 1 do
  (basis[k]:intopois(sin(m*y)), k:k+1)$
for n:2 step 2 thru 1 do
  for m:2 step 2 thru 1 do
    (basis[k]:intopois(cos(n*x)*cos(m*y)),
     basis[k+1]:intopois(cos(n*x)*sin(m*y)),
     basis[k+2]:intopois(sin(n*x)*cos(m*y)),
     basis[k+3]:intopois(sin(n*x)*sin(m*y)), k:k+4)$
k:k-1;
/* Algorithm Steps: 8 and 9 */
/* Generate the determining equations by inner products with basis functions. In the case of
Poisson forms this comes about by stripping off all harmonics of x and y. The stripping occurs
during the succeeding multiplications. */
poistrim(uc,vc,wc,xc,yc,zc) := is (abs(xc) >= 1 or abs(yc) >= 1)$
for i:1 thru k do
  (ns1[i]:poistimes(ns[1],basis[i]),
   ns2[i]:poistimes(ns[2],basis[i]),
   equat[i]:outofpois(ns1[i]),
   equat[k+i]:outofpois(ns2[i]))$
/* Remove the trim function in order not to affect any other operations. */
remfunction(poistrim)$
/* Algorithm Step: 10 */
/* Generate the input parameter lists for the Newton's approximation. */

```

```

/* The function endcons constructs lists by adding to the end of an existing list. */
/* First construct the list of equations to be solved. */
eq1st:[]$
for n:1 thru 2*k do
    (eq1st:endcons(equat[n],eq1st))$
/* Second construct the list of variables to be evaluated. */
vars:[]$
for j:1 thru 2 do
    (vars:endcons(a[j,0,0],vars),
    for n:2 step 2 thru 1 do
        (vars:endcons(a[j,n,0],vars),
        vars:endcons(c[j,n,0],vars)),
    for m:2 step 2 thru 1 do
        (vars:endcons(a[j,0,m],vars),
        vars:endcons(b[j,0,m],vars)),
    for n:2 step 2 thru 1 do
        for m:2 step 2 thru 1 do
            (vars:endcons(a[j,n,m],vars),
            vars:endcons(b[j,n,m],vars),
            vars:endcons(c[j,n,m],vars),
            vars:endcons(d[j,n,m],vars)))$
/* Third set up the initial starting values for the Newton search. */
for j:1 thru 2 do
    (a0[j,0,0]:0.0,
    for n:2 step 2 thru 1 do
        (a0[j,n,0]:0.0,
        c0[j,n,0]:0.0),
    for m:2 step 2 thru 1 do
        (a0[j,0,m]:0.0,
        b0[j,0,m]:0.0),
    for n:2 step 2 thru 1 do
        for m:2 step 2 thru 1 do
            (a0[j,n,m]:0.0,
            b0[j,n,m]:0.0,
            c0[j,n,m]:0.0,
            d0[j,n,m]:0.0))$
a0[1,0,0]:3.53$
a0[2,0,0]:1.18$
init:[]$
for j:1 thru 2 do
    (init:endcons(a0[j,0,0],init),
    for n:2 step 2 thru 1 do
        (init:endcons(a0[j,n,0],init),
        init:endcons(c0[j,n,0],init)),
    for m:2 step 2 thru 1 do
        (init:endcons(a0[j,0,m],init),
        init:endcons(b0[j,0,m],init)),

```

```

for n:2 step 2 thru 1 do
  for m:2 step 2 thru 1 do
    (init:endcons(a0[j,n,m],init),
     init:endcons(b0[j,n,m],init),
     init:endcons(c0[j,n,m],init),
     init:endcons(d0[j,n,m],init)))$
/* Finally call the Newton algorithm. */
/* Print out the variable evaluations at each cycle. */
verbose:true;
/* Use the symbolic Jacobian matrix at each iteration. */
newton_eval_jacobian:1;
/* Turn on the optimization option */
newton_optimize:true;
/* Call the Newton algorithm with an upper limit of 30 iterations. */
newton(eq1st,vars,init,30);

```

7. Discussion of the Residual Error Trends

As ε increases there is clearly a distinct linear trend in the error differences between the numerically computed angular and radial components and the approximate angular and radial components, with both computed on the torus. This is clear from Figures 3 and 6. These trends arise from a linear term that is introduced in the numerical scheme. This term and a superimposed periodic term can be found using a relatively simple analysis of the numerical algorithm involved. A full analysis of Gear's [20] interpolation scheme used to solve the differential equations will not be necessary to identify the terms. A simple Euler scheme will suffice. Furthermore, an analysis of the single van der Pol oscillator will be all that is necessary. The coupled oscillators only introduce complexity but the essential analysis would be the same.

Let h be the same time step used in the numerical algorithm. Let $\theta_n = \theta(t_n)$ and $r_n = r(t_n)$. Then, using a simple difference quotient, (39) can be written for the n -th step case as

$$\begin{aligned}
 \theta_{n+1} &= \theta_n + h + \varepsilon h \Theta(\theta_n, r_n), \\
 r_{n+1} &= r_n + \varepsilon h X(\theta_n, r_n),
 \end{aligned}
 \tag{65}$$

and (48) can be written as

$$\begin{aligned}
 \hat{\theta}_{n+1} &= \hat{\theta}_n + h + \varepsilon h \Theta(\hat{\theta}_n, f(\hat{\theta}_n)), \\
 \hat{r}_{n+1} &= f(\hat{\theta}_{n+1}),
 \end{aligned}
 \tag{66}$$

where f is being used instead of r_ℓ in order not to confuse subscripts. The ‘^’ notation is used to identify the approximate angular and radial results.

The following assumptions can be made. $\theta_n - \hat{\theta}_n$ and $r_n - \hat{r}_n$ are assumed to be small. Figures 3 and 6 show that in absolute terms these errors are small for the simulation time duration. One other assumption that can be made is that, in both cases, using Figures 2 and 5, the radial values can be written as

$$r = \bar{r} + p(\theta)
 \tag{67}$$

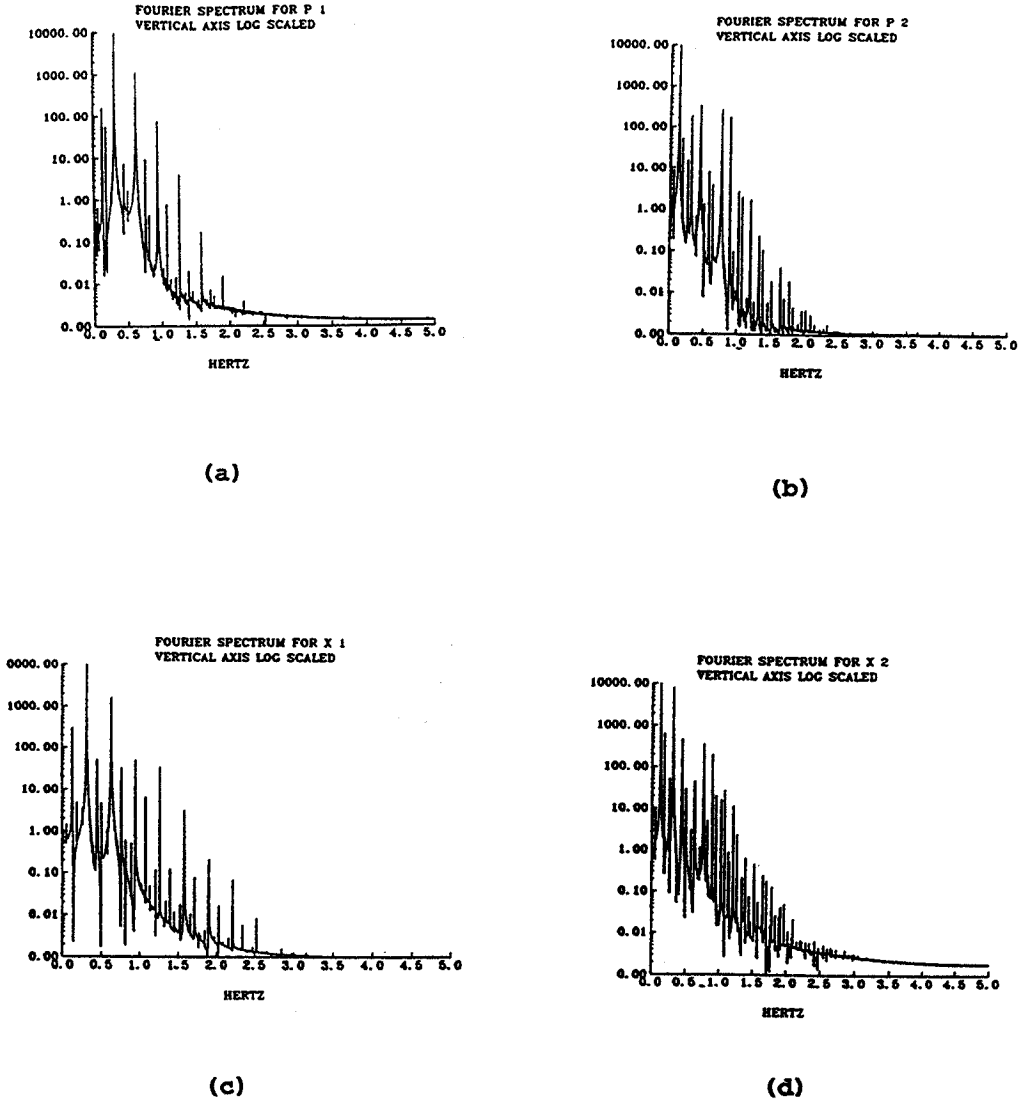


Fig. 7. Spectral plots of the amplitudes of the phase and radial equations for the full system with linear trends removed. Initial conditions as in Figure 5.

where $p(\theta)$ is some bounded periodic function of θ and \bar{r} is the mean radius.

Using first order approximations, the angular and radial differences can be written as

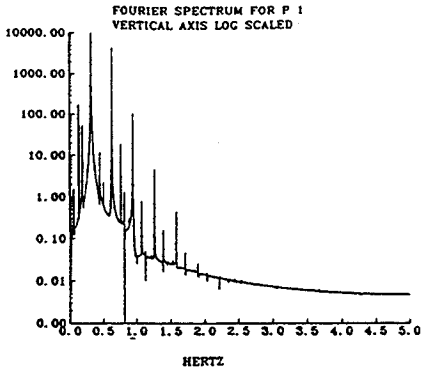
$$\theta_{n+1} - \hat{\theta}_{n+1} \approx (\theta_n - \hat{\theta}_{n+1})(1 + \epsilon h \Theta_1(\hat{\theta}_n, r_n)) + \epsilon h \Theta_2(\hat{\theta}_n, r_n)(r_n - \hat{r}_n) \quad (68)$$

$$r_{n+1} - \hat{r}_{n+1} \approx (r_n - \hat{r}_n) + \epsilon h X(\theta_n, r_n) - f'(\hat{\theta}_n)h - \epsilon h f'(\hat{\theta}_n)\Theta(\hat{\theta}_n, \hat{r}_n) \quad (69)$$

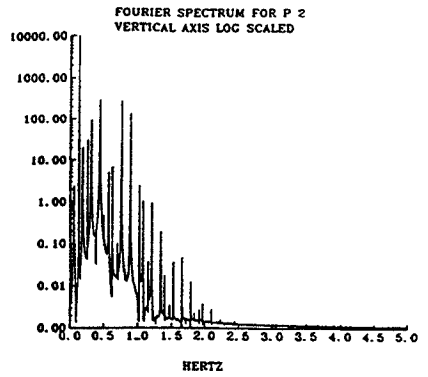
where $\Theta_1 = \frac{\partial \Theta}{\partial \theta}$, $\Theta_2 = \frac{\partial \Theta}{\partial r}$.

Using (40) and (67) one can write

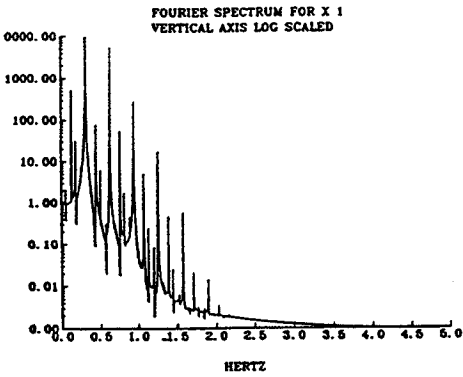
$$X(\theta, r) = \left(\frac{\bar{r}}{2} - \frac{\bar{r}^3}{8} \right) + P_1(\theta),$$



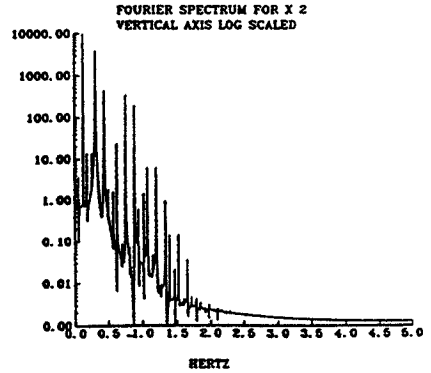
(a)



(b)



(c)



(d)

Fig. 8. Spectral plots of the amplitudes of the phase and radial equations for the approximate system with linear trends removed. Initial conditions as in Figure 5.

$$\begin{aligned}
 \Theta(\theta, r) &= P_2(\theta), \\
 \Theta_1(\theta, r) &= P_3(\theta), \\
 \Theta_2(\theta, r) &= P_4(\theta), \\
 f'(\theta) &= P_5(\theta),
 \end{aligned}
 \tag{70}$$

where P_1, \dots, P_5 have zero averages. After introducing these into (68) and (69) one can write

$$\theta_{n+1} - \hat{\theta}_{n+1} \approx (\theta_n - \hat{\theta}_n)(1 + \varepsilon h P_3(\hat{\theta}_n)) + \varepsilon h P_4(\hat{\theta}_n)(r_n - \hat{r}_n),
 \tag{71}$$

Table 9. Major frequency responses in Hertz after the integration of the full system starting on the torus ($\varepsilon = 0.5$).

$\varepsilon = 0.5$					
Full system integration					
Ang. freq.	Theory	θ_1	θ_2	X_1	X_2
$2\omega_2 - 2\omega_1$	0.132	0.130	0.130	0.130	0.130
-	-	0.185	0.185	0.185	0.185
-	-	-	-	-	0.26
$2\omega_1$	0.318	0.315	0.315	0.315	0.315
$2\omega_2$	0.450	0.4475	0.445	0.445	0.445
-	-	0.5025	-	0.5025	0.5025
-	-	-	0.575	-	0.5775
$4\omega_1$	0.637	0.6325	0.6325	0.6325	0.6325
$2\omega_2 + 2\omega_1$	0.768	0.7625	0.7625	0.7625	0.7625
-	-	0.8175	-	0.8175	-
-	-	-	0.8925	-	0.8925
$6\omega_1$	0.955	0.9475	-	0.9475	-
-	-	-	1.023	-	1.023
-	-	1.0775	1.0775	1.0775	1.0775
-	-	-	-	1.135	-
-	-	-	1.2075	-	1.2075
$8\omega_1$	1.273	1.265	-	1.265	-
-	-	-	1.3375	-	1.3375
$6\omega_2$	1.350	1.395	1.395	1.395	1.395
-	-	-	1.525	-	1.525
$10\omega_1$	1.59	1.58	-	1.58	-
-	-	-	1.655	-	-
-	-	-	1.785	-	-

and

$$\begin{aligned}
 r_{n+1} - \hat{r}_{n+1} \approx & (r_n - \hat{r}_n) + \varepsilon h \left(\frac{\bar{r}}{2} - \frac{\bar{r}^3}{8} \right) + \varepsilon h P_1(\hat{\theta}_n) \\
 & - P_5(\hat{\theta}_n)h - \varepsilon h P_5(\hat{\theta}_n)P_2(\hat{\theta}_n).
 \end{aligned}
 \tag{72}$$

From the definition of P_2 and P_5 the product $P_5(\theta)P_2(\theta)$ can be written

$$P_5(\theta)P_2(\theta) = C_6 + P_6(\theta)
 \tag{73}$$

where P_6 has zero average and C_6 is a nonzero constant. Thus, although P_2 and P_5 have zero averages, their product does not. From (72) and (73), $r_{n+1} - \hat{r}_{n+1}$ can then be written as

$$r_{n+1} - \hat{r}_{n+1} \approx (r_n - \hat{r}_n) + \varepsilon h C_7 + h P_7(\hat{\theta}_n),
 \tag{74}$$

Table 10. Major frequency responses in Hertz after the integration of the approximate phase equations starting on the torus ($\epsilon = 0.5$).

$\epsilon = 0.5$					
Phase equation integration on the approximate torus					
Ang. freq.	Theory	θ_1	θ_2	X_1	X_2
$2\omega_2 - 2\omega_1$	0.132	0.130	0.130	0.130	0.130
-	-	0.185	0.185	0.185	0.185
-	-	-	0.26	-	0.26
$2\omega_1$	0.318	0.315	0.315	0.315	0.315
$2\omega_2$	0.450	0.4475	0.445	0.445	0.445
-	-	0.500	0.500	0.500	0.500
-	-	-	0.5775	-	0.575
$4\omega_1$	0.637	0.630	0.630	0.630	0.6325
-	-	-	-	-	0.7075
$2\omega_2 + 2\omega_1$	0.768	0.7625	0.7625	0.7625	0.7625
-	-	0.8175	-	0.8175	-
-	-	-	0.8925	0.8925	0.8925
$6\omega_1$	0.955	0.9475	-	0.9475	0.9475
-	-	-	1.023	-	1.023
-	-	1.0775	1.0775	1.0775	1.0775
-	-	-	1.2075	1.2075	1.2075
$8\omega_1$	1.273	1.2625	-	1.2625	1.2625
-	-	-	1.3375	-	1.34
$6\omega_2$	1.350	1.395	1.393	1.393	1.393
-	-	-	1.525	1.523	1.523
$10\omega_1$	1.59	1.577	-	1.577	-
-	-	-	1.655	-	1.655
-	-	-	-	1.71	1.7075
-	-	-	1.785	-	1.785

where P_7 has zero average and is periodic. The recursive formula for the radial difference then becomes

$$r_n - \hat{r}_n \approx (r_0 - \hat{r}_0) + (nh)(\epsilon C_7) + h \left(\sum_{i=0}^{n-1} P_7(\hat{\theta}_i) \right). \tag{75}$$

The second term is a linear term with slope ϵC_7 . This explains the linear trend in Figure 3. The third term is a superimposed increasing sum of periodic terms. This explains the superimposed periodicities in Figure 3. The amplitude of the periodicities grow due to the addition at each recursive stage. Note that the slope is a function of ϵ so that for small values the linear slope is not dominant and only begins to show for long simulation times but for larger ϵ the slope becomes dominant almost immediately.

Analyzing the angular error requires introducing (75) into (71). After multiplying through by $P_4(\hat{\theta}_n)$ the first two terms of (75) introduce superimposed periodic terms into (71). The

Table 11. Major frequency responses in Hertz after the integration of the full system starting on the torus ($\varepsilon = 1.0$).

$\varepsilon = 1.0$					
Full system integration					
Ang. freq.	Theory	θ_1	θ_2	X_1	X_2
-	-	0.055	0.055	-	-
$2\omega_2 - 2\omega_1$	0.132	0.1275	0.1275	0.1275	0.1275
-	-	0.1825	0.1825	0.1825	0.1825
$2\omega_1$	0.318	0.310	0.310	0.310	0.310
$2\omega_2$	0.450	0.4375	0.4375	0.4375	0.4375
$4\omega_1$	0.637	0.6175	0.6175	0.6175	0.6175
-	-	0.745	0.745	0.745	0.745
$2\omega_2 + 2\omega_1$	0.768	0.800	-	0.800	0.800
-	-	0.875	0.875	0.875	0.875
$6\omega_1$	0.955	0.9275	-	0.9275	0.9275
-	-	-	1.0025	-	1.0025
-	-	1.055	1.055	1.055	1.055
-	-	1.11	1.13	1.11	-
-	-	1.1825	1.1825	1.1825	1.1825
$8\omega_1$	1.273	1.2375	1.2375	1.2375	1.2375
$6\omega_2$	1.350	-	1.310	-	1.310
-	-	1.365	1.365	1.365	1.365
-	-	1.4925	1.4925	1.4925	1.4925
$10\omega_1$	1.59	1.5475	-	1.6	-
-	-	1.7275	-	1.7275	-
$8\omega_2$	1.80	1.855	-	1.855	-

linear term comes from multiplying $P_4(\hat{\theta}_n)$ times $P_7(\hat{\theta}_{n-1})$ in the last term. P_4 has a $\sin(2\hat{\theta}_n)$ term and P_7 has a $\sin(2\hat{\theta}_{n-1})$ term. But $\hat{\theta}_n = \hat{\theta}_{n-1} + \delta$ where δ is small. Therefore

$$\sin(2\hat{\theta}_n) \sin(2\hat{\theta}_{n-1}) \approx \frac{1}{2} (1 - \cos(4\hat{\theta}_{n-1})) \tag{76}$$

which introduces a nonzero constant. Therefore (71) can be rewritten as

$$\theta_{n+1} - \hat{\theta}_{n+1} \approx (\theta_n - \hat{\theta}_n)(1 + \varepsilon h P_3(\hat{\theta}_n)) + \varepsilon h C_8 + h P_8(\hat{\theta}_n), \tag{77}$$

where $P_8(\theta)$ has a zero average. The recursive formula then becomes

$$\theta_n - \hat{\theta}_n \approx (\theta_0 - \hat{\theta}_0) \prod_{i=0}^{n-1} (1 + \varepsilon h P_3(\hat{\theta}_i)) + (nh)(\varepsilon C_8) + h \sum_{i=0}^{n-1} P_8(\hat{\theta}_i) + O(h^2). \tag{78}$$

Again there is a linear trend term and a superimposed periodic term with increasing amplitude. When ε is small these trends are not dominant but as ε gets larger they become more prominent as noted above. Figures 3 and 6 show the errors beginning at 0. This is because the initial conditions were selected to be the same and the leading terms in (75) and (78) are not present.

Table 12. Major frequency responses in Hertz after the integration of the approximate phase equations starting on the torus ($\varepsilon = 1.0$).

$\varepsilon = 1.0$					
Phase equation integration on the approximate torus					
Ang. freq.	Theory	θ_1	θ_2	X_1	X_2
-	-	0.030	0.030	0.030	0.030
-	-	0.105	0.105	0.105	-
-	-	0.135	0.135	0.135	0.135
-	-	0.165	0.165	0.165	0.165
-	-	-	0.270	0.270	0.270
-	-	0.300	0.300	0.300	0.300
-	-	0.4375	0.435	0.435	0.435
-	-	-	-	-	0.465
-	-	-	0.570	0.5725	0.5725
-	-	0.6025	0.6025	0.6025	0.6000
-	-	0.7375	0.7375	0.7375	0.7375
-	-	0.7675	0.7675	0.7675	0.7675
-	-	-	0.8425	-	0.8425
-	-	-	0.8725	-	-
-	-	0.9025	0.9025	0.9025	0.9025
-	-	-	1.0075	-	1.0075
-	-	-	-	1.0375	1.0375
-	-	1.0675	-	1.0675	-
-	-	-	1.1725	1.1725	1.1725
-	-	-	1.2025	1.2025	1.2025
-	-	-	1.2775	-	-
-	-	-	1.3075	1.3075	1.3075
-	-	1.3375	1.3375	-	1.3375
-	-	-	-	-	1.4725
-	-	1.5025	-	1.5025	-
-	-	-	1.6075	-	1.6075
-	-	-	-	-	1.6375
-	-	1.805	-	1.805	-
-	-	2.105	-	2.105	-

8. Conclusions

This paper has shown that the nonlinear Galerkin variational method, using symbolic expansions, is a viable way of solving the invariant torus equation (11) in the quasiperiodic and periodic case. The symbolic capabilities provided by MACSYMA, through its Poisson series subpackage, provide the necessary efficient representations to manipulate the resulting large trigonometric series generated by the Galerkin technique. From the case studies given in this paper, these tools can adequately handle the computation of parametric representations of limit cycles and invariant tori for van der Pol oscillators. The only limitation is the computing memory accessible to the operating system for the computer used.

This case study of approximating the van der Pol limit cycle and coupled system torus indicates several points about the nature of symbolic approximation. First, to obtain the same maximum error value between the full and approximate system the number of terms required for larger damping parameters grows rapidly. Second, both the full and approximate system integration seem to generate the same frequencies as long as the errors between the systems are not too large. For example, even though the integration of the full system and the approximate system for the coupled oscillators with $\varepsilon = 1.0$ do show similar surfaces the error trends for this case are large. This is reflected in the inability of the approximate system integration to return the same frequencies as the full system integration. Third, the error trends in all cases have an interesting structure. As ε gets larger the errors have distinct trends with superimposed periodicities. These trends are traceable to the numerical approximations used to integrate the differential equations.

Up to this point the current results have emphasized the quasiperiodic nature of the parametric representation of the tori and the trajectories on the tori. As long as a quasiperiodic parametric representation is sought the Galerkin's method demonstrated in this paper shows promise. Its primary limitation is computer memory. However, the more harmonics sought in the tori representation the larger the number of variational equations that need to be solved by Newton's method. As pointed out earlier the size of the algebraic equations solved can become excessively large. Since one of the measures of chaos in a system is a broad-band spectrum it seems clear that the nonlinear Galerkin's method discussed in this paper would become prohibitively expensive in terms of computing resources if it were used to approximate a torus whose Poincaré section is structured as, for example, a homoclinic tangle. As shown in Section 5 even a stable torus whose Poincaré section is a distorted circle is difficult to approximate parametrically.

Acknowledgements

The author wishes to thank Dr. Richard Petti of MACSYMA, Inc. for all of his assistance in introducing the author to the Poisson series subpackage and for the many phone and e-mail consultations on its use. The author also wishes to thank Tim Burns of NIST and the journal referees for their many helpful suggestions.

References

1. Aulbach, B., 'Behavior of solutions near manifolds of periodic solutions', *Journal of Differential Equations* **39**, 1981, 345–377.
2. Barton, D., 'A scheme for manipulative algebra on a computer', *The Computer Journal* **9**(4), 1967, 340–344.
3. Barton, D. and Fitch, J. P., 'Applications of algebraic manipulation programs in physics', *Rep. Prog. Phys.* **35**, 1972, 235–314.
4. Bogoliubov, N. N. and Mitropolsky, Y. A., *Asymptotic Methods in the Theory of Non-Linear Oscillations*, Gordon and Breach, New York, 1961.
5. Brown, H. S., Jolly, M. S., Kevrekidis, I. G., and Titi, E. S., 'Use of approximate inertial manifolds in bifurcation calculations', in *Continuation and Bifurcations: Numerical Techniques and Applications*, Roose, D., De Dier, B., and Spence, A. (Eds.), Kluwer Academic Publishers, Dordrecht, 1990.
6. Carr, J., *Applications of Centre Manifold Theory*, Springer-Verlag, New York, 1981.
7. Debussche, A. and Marian, M., 'On the construction of families of approximate inertial manifolds', *Journal of Differential Equations* **100**, 1992, 173–201.
8. Deprit, A. and Rom, A., 'Lindstedt's series on a computer', *The Astronomical Journal* **73**(3), 1968, 210–213.
9. Deprit, A. and Rom, A., 'Poincaré's continuation by computers', *AIAA Journal* **6**(7), 1968, 1234–1239.
10. Deprit, A. and Rom, A., 'Asymptotic representation of the cycle of Van der Pol's equation for small damping coefficients', *Zeitschrift fuer Angewandte Mathematik und Physik* **18**, 1967, 736–746.

11. Deprit, A. and Schmidt, D. S., 'Exact coefficients of the limit cycle in Van der Pol's equation', *Journal of Research of the National Bureau of Standards* **84**(4), 1979, 293–297.
12. Dieci, L., Lorenz, J., and Russell, R. D., 'Numerical calculation of invariant tori', *SIAM J. Sci. Stat. Comput.* **12**(3), 1991, 607–647.
13. Diliberto, S. P., 'New results on periodic surfaces and the averaging principle', in *Differential and Functional Equations*, New York, 1967, 49–87.
14. Diliberto, S. P., Kyner, W. T., and Freund, R. B., 'The application of periodic surface theory to the study of satellite orbits', *The Astronomical Journal* **66**(3), 1961, 118–128.
15. Fabes, E., Luskin, M., and Sell, G. R., 'Construction of inertial manifolds by elliptic regularization', *Journal of Differential Equations* **89**, 1991, 355–387.
16. Fateman, R., 'On the multiplication of Poisson series', *Celestial Mechanics* **10**, 1974, 243–247.
17. Foias, C., Jolly, M. S., Kevrekidis, I. G., Sell, G. R., and Titi, E. S., 'On the computation of inertial manifolds', *Physics Letters A* **131**(7, 8), 1988, 433–436.
18. Foias, C., Sell, G. R., and Temam, R., 'Inertial manifolds for nonlinear evolutionary equations', *Journal of Differential Equations* **73**, 1988, 309–353.
19. Garcia-Margallo, J. and Bejarno, J. D., 'Generalized Fourier series and limit cycles of generalized van der Pol oscillators', *Journal of Sound and Vibration* **136**(3), 1990, 453–466.
20. Gear, C. W., *Numerical Initial Value Problems in Ordinary Differential Equations*, Prentice-Hall, Englewood Cliffs, New Jersey, 1971.
21. Gilsinn, D. E., 'Asymptotic approximation of integral manifolds', *SIAM J. Appl. Math.* **47**(5), 1987, 929–940.
22. Gilsinn, D. E., 'Constructing invariant tori for two weakly coupled van der Pol oscillators', *Nonlinear Dynamics* **4**, 1993, 289–308.
23. Guckenheimer, J. and Holmes, P., *Nonlinear Oscillations, Dynamical Systems, and Bifurcations of Vector Fields*, Springer-Verlag, New York, 1983.
24. Hale, J. K., 'Integral manifolds of perturbed differential systems', *Ann. of Math.* **73**, 1961, 496–531.
25. Jefferys, W. H., 'Automated algebraic manipulation in celestial mechanics', *Celestial Mechanics* **14**(8), 1971, 538–541.
26. Jolly, M. S., 'Explicit construction of an inertial manifold for a reaction diffusion equation', *Journal of Differential Equations* **78**, 1989, 220–261.
27. Kouda, A. and Mori, S., 'Mode analysis of a system of mutually coupled van der Pol oscillators with coupling delay', *International Journal of Non-Linear Mechanics* **17**(4), 1982, 267–276.
28. Kovalevsky, J., 'Review of some methods of programming of literal developments in celestial mechanics', *The Astronomical Journal* **73**(3), 1968, 203–209.
29. Loud, W. S., 'The location of the invariant manifold for a perturbed autonomous system', *Journ. of Math. and Phys.* **40**, 1961, 87–102.
30. *MACSYMA Reference Manual*, Symbolics Inc., Burlington, MA, 1988.
31. Marion, M. and Temam, R., 'Nonlinear Galerkin methods', *SIAM Journal on Numerical Analysis* **24**, 329–343.
32. Melvin, P. J., 'On the construction of Poincaré–Lindstedt solutions: The nonlinear oscillator equation', *SIAM J. Appl. Math.* **33**(1), 1977, 161–194.
33. Melvin, P. J., 'The phase-shifting limit cycles of the van der Pol equation', *Journal of Research of the National Bureau of Standards* **83**(6), 1978, 593–601.
34. Nayfeh, A. H. and Mook, D. T., *Nonlinear Oscillations*, John Wiley & Sons, New York, 1979.
35. Rand, R. H. and Holmes, P. J., 'Bifurcation of periodic motions in two weakly coupled van der Pol oscillator', *International Journal of Non-Linear Mechanics* **15**, 1980, 387–399.
36. Rom, A., 'Mechanized algebraic operations (MAO)', *Celestial Mechanics* **1**, 1970, 301–319.
37. Sell, G. R. and You, Y., 'Inertial manifolds: The non-self-adjoint case', *Journal of Differential Equations* **96**, 1992, 203–255.
38. Shaw, S. W. and Pierre, C., 'Normal modes for nonlinear vibratory systems', *Journal of Sound and Vibration* **164**(1), 1993, 85–124.
39. Shaw, S. W. and Pierre, C., 'Normal modes of vibration for non-linear continuous systems', *Journal of Sound and Vibration* **169**(3), 1994, 319–437.
40. Stokes, A., 'On the approximation of nonlinear oscillations', *Journal of Differential Equations* **12**(3), 1972, 535–558.
41. Storti, D. W. and Rand, R. H., 'Dynamics of two strongly coupled van der Pol oscillators', *International Journal of Non-Linear Mechanics* **17**(3), 192, 143–152.
42. Urabe, M., 'Galerkin's procedure for nonlinear periodic systems', *Arch. Rat. Mech. and Anal.* **20**(2), 1965, 120–152.
43. Wang, S. and Huseyin, K., 'MAPLE analysis of nonlinear oscillations', *Math. Comput. Modelling* **16**(11), 1992, 49–57.
44. Whittaker, E. T., *A Treatise on the Analytical Dynamics of Particles and Rigid Bodies*, Dover, New York, 1944.

